# By precisely describing the planetary conditions and related properties of habitable exoplanets, AI algorithms can improve their identification and analysis.

*Harshika Kerkar, Jahanvi Chamria, Riddhim Garg*

# Table of Contents

## Abstract

This research focuses on the application of Artificial Intelligence (AI) to identify and evaluate the potential for habitability of exoplanets. It aims to train AI models capable of filtering exoplanets from a given dataset and further categorizing their potential for habitability on a scale depending on various planetary conditions. It questions how various crucial factors such as the radiative flux and the eccentricity of a planet affect its ability to support life. To achieve these goals, various AI models were systematically tested and the highest accuracy (~97%) was achieved using a Random Forest Classifier for both exoplanet detection and habitability potential. The study also discusses the importance of the Habitable Zone and liquid water in sustaining life. The data used is from NASA's Kepler Cumulative dataset. The research highlights the benefits of employing AI models to assess large datasets of exoplanets for the exploration of distant planetary systems.

# 1. Introduction

The discovery of exoplanets has long been a focus of the space research community. The basic premise behind it is the prospect of discovering habitable planets or extraterrestrial life. This research will investigate the atmosphere and other features of exoplanets that help us designate them as habitable exoplanets. Based on these qualities, we will employ artificial intelligence to improve planet detection and analysis.

To begin, we will need to understand the fundamentals of exoplanet sciences and astrobiology in order to provide the groundwork for what follows. Then we'll look into exoplanet detection and atmosphere analysis techniques. Furthermore, we will analyse the criteria and circumstances for habitability in order to comprehend how a planet is considered habitable. Because the atmosphere is so important in assessing a planet's habitability, exoplanet atmospheric composition and models will be covered. Continuing, the goal of this study is to use artificial intelligence to find and characterise exoplanets and their atmospheres so, we will also investigate the prior use of artificial intelligence in detecting exoplanets. Finally, significant technological and scientific achievements in the history of exoplanet detection will be highlighted.

# 2. Theory

## 2.1. Basics of Exoplanet Science

### 2.1.1. Definition of Exoplanets

An exoplanet, short for extrasolar planet, is a celestial body that orbits a star outside the confines of our solar system. This notion, once the topic of philosophical debates, has become one of the most revolutionary fields in modern astronomy. The thought that our solar system might not be singular, and that other stars might harbor their own set of planets, has a long and storied history. Notably, Dominican Friar Giordano Bruno posited in his 1584 work "De l'Infinito, Universo e Mondi" that the night sky's stars could very well be suns with their own planets orbiting them. He posited that these worlds remain invisible to us due to their diminutive size and faintness compared to their host stars, a challenge that persisted for centuries and that modern astronomers are only now beginning to overcome [1].

The preliminary strides toward exoplanet detection transpired in the 18th and 19th centuries, through observations that anticipated modern exoplanet detection techniques. One such observation by British astronomer John Goodricke in 1783 revealed that periodic dimmings of the star Algol were caused by an unseen companion orbiting it [2]. This laid the groundwork for the exoplanet transit technique used today.

The 20th century witnessed claims, later debunked, of exoplanet discoveries based on observed wobbles in star movements. The authentic breakthrough in exoplanetary science occurred in the late 1980s and early 1990s with discoveries around stars such as Gamma Cephei A and HD 1146723 [3]. What followed was an outpouring of discoveries, including planets orbiting pulsars and the "first planet around a Sun-like star" - 51 Pegasi b [4].

Contrary to prior assumptions that planetary systems would mirror our solar system, the first exoplanet discoveries ushered in a realization: the diversity and variety of planetary systems is staggering. The cosmos teems with planets on eccentric orbits, planets denser than any material we know, and planets so light they could be likened to fairy floss [5]. This immense diversity underscores the complexity and richness of our universe.

#### 2.1.2. Importance of Studying Exoplanets

The study of exoplanets, planets that orbit stars outside our solar system, serves as a cornerstone for multiple scientific disciplines, providing insights that extend beyond planetary science into the realms of astrophysics, astrobiology, and even philosophy [6].

#### 2.1.3. Astrobiology and the Search for Extraterrestrial Life

One of the most captivating prospects of exoplanetary science is its potential to answer the age-old question: Are we alone in the universe? Recent advancements in exoplanetary studies have made it conceivable to detect bio-signatures—indicators of biological activity—in the atmospheres of exoplanets within the next decade [6]. This drives the field of astrobiology, aiming to understand life's potential to arise elsewhere in the universe [7].

#### 2.1.4. Understanding Planetary Formation and Diversity

Studying exoplanets also enables scientists to test theories of planetary formation. The recent surge in discovered exoplanets has showcased a rich diversity of planetary characteristics and systems, radically different from our own solar system [8]. Understanding this diversity helps to enrich and challenge existing theories of planetary formation [9].

#### 2.1.5. Comparative Planetology

The field of comparative planetology has also greatly benefited from exoplanetary studies. By comparing the geological and atmospheric characteristics of planets in our solar system with those of exoplanets, we can form a comprehensive understanding of planetary processes [10].

#### 2.1.6. Stellar Evolution

Studying the interactions between exoplanets and their host stars can offer invaluable insights into stellar evolution processes. Exoplanets and their stars often exert mutual influences that are crucial for understanding both planetary and stellar life cycles .

#### 2.1.7. Technological Advancements

The need to detect and study distant planets has spurred significant technological innovations, especially in the field of astronomy. Advanced telescopes and detection methods, some solely dedicated to exoplanetary research, are among these advancements [11].

#### 2.1.8. Philosophical and Societal Implications

The discovery of extraterrestrial life would raise profound questions about human significance, spirituality, and the ethics of interacting with other sentient beings [12].

#### 2.1.9. Planetary Habitability and Resources

As our own planet faces increasing resource constraints, understanding the conditions that could support life elsewhere could have direct implications for the future of humanity [13].

#### 2.1.10. Milestones in Exoplanet discovery

2.1.10.a. Over 1,200 new planets have been confirmed by NASA's Kepler mission, making it the greatest planet discovery to date [14].

2.1.10.b. The two years with the largest exoplanets discoveries were: 875 planets discovered in 2014 and 1,517 planets discovered in 2016 [14].

2.1.10.c. As per now, over 5,000 planets have been discovered, out of which, over 4000 planetary systems are present with more than 9,000 candidates [14].

2.1.10.d. Historic Timeline of Exoplanet discovery [15]:

April 1984: First planetary disk observed

April 23, 1990: Hubble Space Telescope is launched

January 1992: First exoplanets are discovered

October 1995:First exoplanet around a main-sequence star is discovered

1999: First transiting exoplanet discovered and first multi-planet system is discovered

April 4, 2001: First planet within the habitable-zone found

October, 2001: First measurement of an exosolar planet's atmosphere

March 2005: First light from exoplanet observed

May 2007: First map of an exoplanet created

March 6, 2009: Kepler planet-finding mission launches

September 2013: First exoplanet cloupmap created

April 2014: First Earth-sized exoplanet in the habitable zone discovered, Kepler-186f

February 2017: Seven Earth-sized planets found orbiting a red-dwarf star, TRRAPIST-1

December 2017: Eight planet was discovered in the Kepler-90 system using Artificial intelligence.

April 18, 2018: Launch of the TESS mission.

December 25, 2021: The launch of James Web Space Telescope.

## 2.2. Exoplanet Detection Methods and Characterization

### 2.2.1. Transit Photometry

#### 2.2.1.a. Description and Mechanism

Transit photometry is a robust method for detecting exoplanets by monitoring the brightness of stars for periodic, short-lived dimming events, indicative of a planet transiting across the parent star's disk [16]. This transit blocks a small fraction of the star's light, allowing for the potential discovery of the planet. High-precision follow-up observations can yield a wealth of additional data, including planetary mass, radius, and mean density, that are otherwise unavailable for non-transiting planets [17].

#### 2.2.1.b. Key Aspects of Transits:

i. The transit probability. Transits are rare because the planetary orbital plane must be nearly edge-on as viewed from Earth. For randomly oriented orbits this circumstance occurs with a probability of approximately  where R* is the stellar radius and r is the planet-star distance at the time of conjunction. For a Sun-like star, the probability is ~0.5% for r = 1AU and ~10% for r = 0.05AU.

ii. The transit depth. During a transit, a fraction of the starlight is blocked. For a Sun-like star, this fraction is 1% for a Jovian planet and 8x10-5 for an Earth-sized planet

iii. The transit duration. The transit lasts for a duration ~ where is the orbital velocity of the planet. The exact duration also depends on the impact parameter of the planet's trajectory across the stellar disk. For a Sun-like star, the transit of a close-in planet with r = 0.05AU lasts ~2hr, while the transit of a more distant planet at 1AU lasts ~12hr [16].

2.2.1.c. Number of Exoplanets Detected and Current State of the Art

The advancements in the field of exoplanetary science over the years have led to significant strides in the detection and characterization of exoplanets. The discovery of approximately two dozen transiting exoplanets has transformed our understanding, as these planets are the only ones that can be comprehensively characterised using current technology. This characterization encompasses measurements of their physical mass, radius, temperature, and atmospheric composition [16].

A groundbreaking finding is the ability to determine a planet's bulk density by using transits that are coupled with radial velocity or astrometric studies to determine the planet's mass. The importance of this combined analysis becomes evident when considering the thirty transiting hot Jupiter exoplanets; their combined masses and radii have provided data that challenges our existing theories on planet formation and evolution [16].

Furthermore, when considering stars like M-dwarfs, the search for exoplanets becomes even more promising. Their habitable zone is closer, thus increasing both the probability of transits and the radial velocity amplitude, making the search for Earth-like planets in the habitable zone more attainable [16]. Ground-based systems, along with proposed space-based systems, can conduct transit surveys of numerous nearby M-dwarfs, enhancing the possibility of detecting a habitable planet in the coming decade.

The Spitzer telescope has been a pivotal instrument in advancing exoplanet science, especially in the realm of comparative exoplanetology, through its transit observations. For instance, it's been used to determine temperatures of various Jupiter-mass exoplanets, interpret thermal orbital phase curves, and even identify the presence of water vapor [16]. A key aspect is that the Spitzer telescope, even after its cryogenic mission has ended, remains unparalleled in studying transiting planets through temperature and spectral readings, at least until the launch of the James Webb Space Telescope (JWST).

The future promises even more advancements with the JWST. Designed with capabilities to conduct transit studies of Earth-sized planets in the habitable zones of M-dwarfs, it could provide us with the first detailed characterization of a true Earth analog orbiting an M-dwarf [16].

Lastly, the Kepler Mission stands as a crucial endeavour to understand the frequency of Earth-sized planets around solar-type and other main-sequence stars. This will help in

understanding if Earth-sized planets are a common result of star formation, and thus the likelihood of similar planets within our solar neighborhood. Before Kepler's achievements, ground-based surveys targeting M-dwarfs may also help gain insights into short-period transiting planets nearing Earth's size [16].

2.2.1.d. Limitations

Transit photometry has undeniably propelled our understanding of exoplanets, revealing diverse worlds and intricate planetary systems. However, it is essential to recognise the inherent constraints of this method to ensure a comprehensive appreciation of its findings:

i. **Geometric Probability:** The method primarily hinges on the geometric alignment of the star, planet, and the observer. Specifically, the probability of a planet transiting its star is governed by the relation where $R_*$ denotes the stellar radius and $a$ the planet-star separation. This means that many exoplanets, if not perfectly aligned with our perspective, remain undetected by this method alone [18].
ii. **Observation Duration:** Confirming the presence of smaller planets necessitates prolonged observations, often employing the most massive ground-based telescopes equipped with highly stable spectrographs. This time-intensive requirement can pose significant operational challenges [19].
iii. **False Positives and Stellar Activities:** Stellar phenomena, such as star spots, or even other stellar bodies, can imitate transit signals. This propensity to produce false positives necessitates meticulous follow-up observations to verify the existence of an exoplanet.
iv. **Limited Characterization:** While transits can divulge atmospheric characteristics, this is primarily efficient for larger planets with extensive atmospheres. Characterizing Earth-sized planets or those with sparse atmospheres remains a challenge. Existing technology largely confines the physical characterization of planets to those transiting their stars [20].
v. **Bias Towards Specific Star Types:** Ground-based transit surveys predominantly focus on nearby M-dwarfs. Although they possess a higher probability of harbouring transiting planets due to their size and habitable zone proximity, such stars' inherent stellar activities can introduce interpretative complexities.
vi. **Statistical Limitations:** The number of transiting planets discernible around luminous stars is fundamentally circumscribed by statistics, affecting the practicality of subsequent characterization [18].
vii. **Large Sample Sizes:** Due to the geometric challenges and the vastness of space, astronomers need to monitor an expansive number of stars to identify a substantial number of transiting exoplanets.
viii. **Orbital Radius Constraints:** The likelihood of detecting a transit dips as the planet's orbital radius grows. This inherent limitation complicates the discovery of planets in more distanced orbits around their host stars [17].

ix. **Distance and Brightness Limitations:** Stars monitored by certain missions, like Kepler, are far away. This distance complicates follow-up techniques like Doppler velocimetry essential for characterizing discovered exoplanets. Brightness also plays a crucial role as dim stars make the detection process more intricate [17].

### 2.2.2. Radial Velocity

The Radial Velocity (RV) method, also known as Doppler spectroscopy, is a predominant technique for detecting exoplanets. It capitalises on the gravitational interactions between a planet and its host star, leading to observable Doppler shifts in the star's light spectrum.

#### 2.2.2.a. Principles of the Radial Velocity Method

Stars and their planets do not orbit a fixed point within the star. Instead, both the star and its planet orbit around a common center of mass. This dynamic induces a reflex motion in the star, a periodic oscillation detectable from Earth. When the system's orientation is nearly edge-on relative to Earth, the star's motion toward and away from Earth manifests as an oscillating Doppler shift. This results in the star's atomic and molecular spectral lines shifting slightly toward the blue (blue-shift) when the star is moving towards Earth and then to the red (red-shift) when it is moving away [16].

Essentially, Doppler-shift spectroscopy measures only the component of a star's to-and-fro motion along our line of sight. This "radial" component of the star's motion creates the aforementioned Doppler shift. Modern telescopes, when equipped with precise spectrometers, can identify radial velocities as subtle as a few meters per second, equivalent to a walking speed, which causes a Doppler shift of a part in $10^8$ of the spectral line's wavelength [17].

Initially, the method was most efficient at detecting massive planets close to their host stars. This is because such planets induce larger reflex velocities in their host stars. However, with advancing technology and prolonged observation times, the technique's precision has increased. This progression has allowed for the discovery of planets of lesser mass and at greater orbital distances. Recent statistics from Doppler surveys suggest [16]:

i. About 1% of Sun-like stars host very close gas giant planets, known as hot Jupiters.

ii. Gas giant planet formation appears more efficient around high metallicity stars.

iii. A minimum of 15% of stars possess gas-giant planets with orbital periods under 10 years.

iv. Around 50% of stars with one identified planet exhibit additional velocity variations, hinting at the existence of more planets.

v. There is an upward trend in planet numbers as planetary mass decreases.

2.2.2.b. Radial Velocity Findings

Among the various techniques employed for exoplanetary discovery, radial velocity stands out as the foremost method in the quest to detect low-mass planets in the vicinity of stars.

The pursuit for precision in radial velocity measurement is ever-advancing, with 1 m/s currently being the benchmark and the ambitious goal set at 0.1 m/s. This drive i's pivotal for detecting Earth-like planets. The report documents a notable discovery of a planet with M sin i of 5.1 $M_{\oplus}$, a result of achieving an impressive 0.6 m/s precision. There is a noticeable bottleneck in accessing premier radial velocity instruments. This limitation becomes even more pronounced given the forthcoming influx of potential exoplanetary candidates from missions like Kepler. The technique showcases its potential in detecting terrestrial-mass planets, particularly around low-mass stars. The method can uncover significant numbers of exoplanets with M sin i measurements as low as 10 $M_{\oplus}$, especially when associated with solar-type stars located in the habitable zone. M-dwarf stars, main sequence ones in particular, are intriguing targets. A given radial velocity precision can detect a planet of lower mass around an M star as compared to a G star. However, observing the less luminous M-dwarfs requires shifting from visible-wavelength techniques to near-infrared Doppler spectroscopy, a technology currently being refined [16].

### 2.2.3. Gravitational Microlensing

Gravitational microlensing stands as one of the most intriguing methods to detect exoplanets. Its underlying principle is grounded in Einstein's theory of general relativity, which predicts that massive objects can bend and focus the light from objects behind them.

2.2.3.a. Mechanism of Microlensing:

When a star (referred to as the lens) passes nearly directly in front of a more distant star (the source), the gravitational field of the lens focuses the light from the source, producing two images on opposite sides of the lens. Typically, these images are separated by a minuscule ~1 milliarcsecond (mas), rendering them mostly unresolved. However, the magnification due to lensing leads to a perceivable brightening and dimming of the source star in a characteristic bell-shaped light curve [16].

2.2.3.b. Revelation of Planets:

If the lens star hosts a planet, this planet can substantially perturb this light curve if it comes close to one of the created images, thus revealing its existence. Post-event observations often allow scientists to characterize the host star sufficiently to discern the

mass of the planet and its projected separation from the star in actual physical units [17].

#### 2.2.3.c. Microlensing's Strength:

The theoretical framework of microlensing is rigorous. Utilizing space-based surveys, it becomes possible to ascertain the occurrence of planets based on their mass (down to 0.1 Earth masses), the type of their host star, and the planet's separation from its star ranging from 0.5 to 15 Astronomical Units (AU) [21]. Notably, planets beyond this range might blur into the category of free-floating planets.

#### 2.2.3.d. Microlensing Findings

Among the microlensing-detected planets, two are categorized as cold Neptunes, while the remaining four fit the cold Jovian mold. Intriguingly, two of these Jovian planets belong to a system strikingly reminiscent of our Jupiter-Saturn setup, sharing analogous mass ratios, separation metrics, and thermal profiles. These observations lead to two pivotal conclusions [16]:

- Cold Neptunes are relatively common in our galaxy.
- Solar system analogs, with configurations similar to ours, might not be rare.

Furthermore, microlensing stands out as the sole method capable of identifying old, free-floating planets. Microlensing's potential can be realized with modest investments in ground-based initiatives. A single dedicated 2-meter class telescope can boost the method's planet detection efficacy, building on the last decade's significant microlensing strides. For a comprehensive statistical planetary overview in the Galaxy, encompassing a range of plausible semi-major axes, a space-based microlensing strategy is paramount, possibly feasible through a Discovery-class mission.

## 2.3. Spectroscopic Techniques for Atmospheric Analysis

The light coming from an exoplanet's atmosphere is captured by telescopes and split by spectrometers. The "black bars" in the rainbow spectrum indicate that the corresponding wavelength of light has been absorbed by the gases in the planet's atmosphere, revealing their presence [22]. In this way, the chemical composition of the atmosphere can be understood to determine habitability [23]. However, there exist limitations due to the faintness of the light obtained which can be $10^{-3}$ to $10^{-5}$ as intense as light coming from the host star. The influence of the star cannot usually be wholly eliminated, modifying the measurement [24].

### 2.3.1. Transmission Spectroscopy

During a planetary transit in front of its star, some light may pass through the planet's atmosphere on its way to the Earth. The light emerges from the planetary atmosphere after passing through varying depths of the atmosphere. This is the most widely-used

method. The measurement of the total brightness of the star and planet combined over time is called the transit light curve. In transit, the planet may block a small fraction of the stellar flux which is equal to the projected area of the planet relative to the area of the star. This drop in flux is known as the transit depth which is wavelength-dependent. At wavelengths where the atmosphere is more opaque, the planet blocks more stellar flux due to absorption by atoms or molecules. A disadvantage of this technique is that only a small fraction of the light passes through the planet's atmosphere. As a result, very careful calibration and data reduction needs to be performed. However, an advantage of this technique is that a transit only lasts a few hours so very often the in-transit and out-of-transit calibration comparison data can be acquired in a single session in one night [25].

Theoretical models for the spectrum require calculation for the light on the slant path passing through the planetary atmosphere. A rough estimate can be made based on the atmosphere scale height . It is the change in altitude over which the pressure drops by a factor of . Using the ideal gas law and assuming hydrostatic equilibrium [26],

$$H = \frac{K_b T_{eq}}{\mu g}$$

($K_b$ is the Boltzmann constant, $T_{eq}$ is the planet's equilibrium temperature, $\mu$ is the mean molecular mass, $n$ is the number of scale heights crossed at wavelengths with high opacity and g is the surface gravity).

The amplitude of spectral features is then:

$$\delta_\lambda = \frac{(R_p + nH)^2}{R_s^2} - \frac{R_p^2}{R_s^2} \approx 2nR_p H/R_s^2$$

Hence, the ideal candidates for this method have high equilibrium temperatures, small host stars, low surface gravity and are hydrogen-dominated. Even in such cases, the amplitude of spectral features is only

### 2.3.2. Thermal Emission Spectroscopy

If an exoplanet or its atmosphere is hot enough, it may emit blackbody radiation which can be detected. The host star and exoplanet can both be treated as blackbodies and the ratio of their fluxes can be found out. The dominant source of thermal emission is the re-radiation of incident stellar flux. The size of the emission signal can be predicted from the planet's equilibrium temperature:

$$\frac{F_p}{F_s} = \frac{B(\lambda, T_{eq})}{B(\lambda, T_s)}\left(\frac{R_p}{R_s}\right)^2$$

If the temperature increases with altitude, spectral features are visible in emission rather than absorption. Thermal emission spectroscopy is useful in understanding the temperature structure along with atmospheric composition.

#### 2.3.3. Reflection Spectroscopy

At any point in an exoplanet's orbit but especially close to the secondary eclipse (occultation), light from its star may bounce off the exoplanet's atmosphere and be directed towards the Earth. The reflected light can subsequently be separated from that of the host star and analyzed, especially at short wavelengths. The reflected light can be quantified in terms of – The ratio of reflected light from a fully illuminated planet relative to reflection from a flat, perfectly diffusing disk with cross-sectional area equal to that of the planet. The total reflected light signal then is,

$$F_{reflect} = A_g(R_p/a)^2\phi(\alpha)$$

This technique is difficult as it requires detecting faint reflected light and breaking it up into its spectrum, as compared to bright light from the host star. Hence, it might be better to use optical photometry – low-resolution spectroscopy using ranges hundreds or thousands of Angstroms wide. Using this method, Earth-like planets could be separated from others using just three broad passbands (red, green and blue).

#### 2.3.4. General trends observed in exoplanet atmospheres

Commonly found molecules and atoms detected in exoplanetary atmospheres include $H_2O$, CO, $CH_4$, $NH_3$, $CO_2$, HCN, $C_2H_2$, H, He, Na, K, Li, Mg, Ca, Fe, V, Cr etc. It has also been found that most atmospheres are cloudy or hazy. These aerosols limit our ability to determine the exact chemical composition of these atmospheres. The particles produce flat and featureless spectra and are a result of either condensation of atmospheric species when the partial pressure of vapour exceeds the saturation vapour pressure or photochemical hazes resulting in the formation of involatile solids. Their effects must be taken into account when analyzing the spectra or retrieving molecular abundances and thermal structures of exoplanetary atmospheres [26, 27].

### 2.4. Criteria for Habitability (Parameters for Potentially Habitable Exoplanets)

Currently, our understanding of habitability is limited to the conditions present on Earth. They are often rated on the Earth Similarity Index (ESI). Using this Earth-based criteria, several potentially habitable exoplanets have been hypothesized. However, these are much lesser in number compared to the list of non-habitable exoplanets. Hence, they can be thought of as anomalies in a large group of non-habitable instances. Since the

Earth is the only known habitable planet, life can be thought to be arbitrarily rare. We can characterize exoplanets in terms of different parameters based on the conditions present on Earth and screen these anomalies from all other exoplanets detected [28].

### 2.4.1. Stellar Type and Stability

In addition to the requirements of liquid water and climatic conditions, there are certain important conditions an exoplanet needs to fulfill in order to be qualified as potentially habitable. These are influenced largely by a broad range of stellar, orbital and planetary properties that are different from the terrestrial requirements. The key driver of an exoplanet's environment is the host star. The insolation i.e. the radiative flux a planet receives from its host star is an important factor in determining the surface conditions and climate. Along with the spectral energy distribution (SED) of the host star, the insolation is also used to define the spatial extent of the habitable zone (HZ). It is also important to note that habitable planets may exist in binary or multiple-star systems too. A relatively large number of planets have been discovered in binary stellar systems, both circumstellar and circumbinary [29]. The habitable zone (HZ) around a star is typically defined as the region where a rocky planet can maintain liquid water on its surface. The inner edge of the HZ is dependent on how warm the planet can get in that zone. Two cases may occur: (i) runaway greenhouse in which the surface temperature exceeds the critical temperature for water (647 K) and the entire ocean evaporates or (ii) moist greenhouse in which the surface temperature exceeds ~340 K for a 1-bar Earth-like atmosphere, causing the $H_2O$ saturation mixing ratio at the surface to exceed 0.2. This leads to large increases in tropospheric and stratospheric heights, so water can rapidly photodissociate and be lost to space. The outer edge can also be defined on the basis of the maximum greenhouse effect: the distance at which warming by $CO_2$ reaches a maximum and the solar flux required to maintain a 273 K surface temperature reaches minimum value. Additionally, some authors have suggested modifications of these HZ boundaries based on other factors like the presence of other greenhouse gases [30]. Many newly discovered exoplanets orbit stars cooler compared to the Sun because the habitable zones corresponding to such stars are easier to detect. However, they often have increased activity compared to the Sun including flaring, coronal mass ejections (CMEs) and active magnetic fields. Stellar flares are related to increased UV and charged particle flux but these conditions do not affect habitability. However, the increased likelihood of CMEs can affect habitability due to atmospheric erosion or compression of planetary magnetospheres [31].

### 2.4.2. Orbital Characteristics and the Goldilocks Zone

It was believed that the conditions required for life to be present on another planet needed to be near perfect compared to Earth. These conditions, including atmospheric oxygen and liquid water, have led researchers to look for habitable exoplanets in the Goldilocks zone or a part of space in which a planet is at the optimal distance from its host star, allowing for a surface temperature that is neither too hot nor too cold. However, these conditions have been redefined over the years because sometimes life

can survive in extreme environments too. The Goldilocks zone is also known as the habitable zone or HZ [32]. The rate of rotation of a planet has a significant effect on atmospheric circulation, the efficiency of latitudinal heat transport, cloud distributions, precipitation patterns and surface temperatures. The number and latitudinal extent of wind are determined by the strength of the Coriolis effect which is determined by the rotation time period. The rotation time period is in turn dependent on the evolutionary path and frequency of encounters with exchanges in angular momentum, including star-planet and planet-moon tidal dissipation [33]. Another important factor affecting habitability is the eccentricity. If a planetary orbit is too eccentric it might lead to absence of liquid water all year round as the planet moves closer and farther to its host star. Obliquity is the tilt of the planet's rotation axis [34]. Less tilt leads to stable temperatures and prevention of extreme weather patterns. Linsenmeier et al. (2015) studied the influence of both obliquity and eccentricity for ocean-covered planets orbiting a Sun-like star on a 365-day orbit and a 24-hour day, similar to Earth. It was found that planets with eccentricities higher than 0.2 can only sustain surface liquid water for a certain part of the year. Of the planets on NASA's exoplanet archive, only 21.7% of the planets could potentially sustain liquid surface water year round [35]. The orbital stability is also an important factor in determining habitability. More massive planets have higher gravitational forces and orbit closer to their host stars which makes them more likely to be tidally locked, having one side always facing the star. This results in extremely hot or cold conditions and may affect life forms. However, planets with lower masses have weaker gravitational forces and less resistance against disturbances caused by external bodies nearby, increasing the likelihood of unstable orbits and ejection into space over time [36].

### 2.4.3. Planetary Mass and Gravity

Planetary mass plays a prominent role in determining whether a planet can support life. The mass determines its size, density and atmospheric pressure which affects temperature regulation on its surface. Larger planets have stronger gravitational forces that help retain their atmospheres over a long period of time, creating better atmospheric pressure for complex life forms to exist. However, very large gravitational forces also hinder the development of life by creating inhospitable environments. On the other hand, lighter planets may lose their atmospheres owing to hydrodynamic escape. The gravity affects climate cycles and even geology depending on its strength. It has two main effects on habitable planets: (i) strong gravitational forces help retain the atmosphere by preventing gas molecules from escaping into space over time and (ii) stronger gravity creates stronger tidal effects like ocean tides, causing geological activity like volcanic eruptions and earthquakes which can allow for the creation of more dynamic environments with diverse ecosystems. Overall, the planetary mass and gravity also affect the surface temperature. Larger planets having higher mass and stronger gravity have thicker atmospheres trapping more heat from the host star and resulting in higher temperatures [36].

### 2.4.4. Atmospheric Conditions

#### 2.4.4.a. Factors Influencing Atmospheric Chemistry of Exoplanets

The discovery of a vast diversity of exoplanets, many of which have no analogues in the solar system, has revolutionized astronomy. This diversity suggests an exoplanet zoo with a wide range of sizes, atmospheric temperatures, and elemental compositions. Theorists must understand the variety of existing planetary climates. To infer the chemical composition of exoplanet atmospheres, a theoretical approach must identify and understand the impact of various parameters on atmospheric chemistry [37].

i. Gravity

The planet's mass and radius, derived from radial velocity and transit techniques, determine its ability to retain atmosphere. Gravity and host star X-ray and EUV flux [38] also influence atmospheric composition. Gravity, along with particle mass and temperature, sets the scale height of the atmosphere, determining its compactness or extension.

ii. Elemental composition

The atmospheric composition of planets is influenced by the relative abundances of elements. Giant planets, due to core accretion, can capture nebular gas efficiently, retaining a thick H/He-dominated atmosphere. Terrestrial planets, on the other hand, do not, and their atmospheres depend on their mass and evolutionary history. Terrestrial atmospheres are typically dominated by secondary products like $H_2O$, $CO_2$, CO, $N_2$, Ne, Ar, Kr, $SO_2$, and $SiO_2$. A regime of super-Earths/sub-Neptunes with unknown elemental composition is between giant and terrestrial planets. Comparing chemical models and observations can constrain the elemental composition of the atmosphere, providing insights into the planet's formation and evolution [37].

iii. Insolation

The energy received at the top of the atmosphere is influenced by the host star's luminosity and orbital distance, which can be constrained by observations. The spectral type of the star also affects atmospheric characteristics. Incoming visible and infrared photons heat the atmosphere, while ultraviolet photons heat the high-altitude thermosphere [37].

iv. Internal heating

Planets' interiors generate significant atmospheric heat, influenced by their age and tidal interactions with the host star or other planets. Estimates are based on theoretical models, but uncertainties in key factors like bulk material dissipation and star age limit the accuracy of these estimates [37].

v. Solid surfaces

Life thrives at discrete interfaces [39], especially on rocky and icy planets, and is more favored on substrates protected from shortwave [40] and charged particle radiation [41].

Habitability on planets is influenced by solid substrates, which offer stability, chemical compound density, and protection from radiation. Rocky planets and planets with frozen layers provide interfaces for organisms and nutrients. Planets with solid cores generate internal heat from radioactive decay, and regenerative biosphere recycling [42, 43] is essential for stabilizing the climate. Habitability correlates positively with solidity, with rocky or frozen substrates indicating a positive correlation [44].

vi. Atmosphere

An atmosphere on planets promotes habitat by protecting the surface from shortwave radiation, stabilizing surface liquids, shielding surface liquids against photolysis, maintaining barometric pressure against boiling, and allowing an exchange medium for gaseous metabolites [40, 45, 46]. It also provides a tropopause cold trap, preventing water loss and hydrogen escape [47]. The size of an atmosphere on exoplanets can be evaluated using the Total Planetary Footprint (TPF) and enhanced imaging technologies. The planetary bond albedo is determined using long-term photometric observations [48, 49].

vii. Magnetosphere

Magnetic fields enhance habitability on terrestrial surfaces by deflecting radiation and providing energy for living organisms. However, the yield of free energy is small [144, 148]. Measurement of magnetospheres at great distances may be challenging, but promising techniques have been proposed [51, 52].

### 2.4.5. Energy Availability

Sunlight and chemistry are the most effective sources of free energy for driving biological processes on planetary bodies near the sun [53-55]. Heat, while commonly available, is inefficient and non-regenerative [50]. Tidal flexing, a common source of heat on solid bodies, could contribute significantly to habitability due to cyclic variations in gravity.

i. Light

The stellar flux received by a planet is an inverse function of the square of the distance of that body's orbit from its central star and depends further on the luminosity of the star. We assume that light up to a distance of 2.5 AU from our Sun can support photosynthesis well and that photosynthesis can be driven to some degree at distances at least up to 10 AU [56].

ii. Heat

Heat can be harvested for living processes on worlds without efficient energy sources [50, 57]. It affects the environment's habitability, as low temperatures dampen chemical reactions and high temperatures destabilize complex molecules. Planets with mean surface temperatures between 200 and 400 K have a 1 value. On Venus, near-infrared windows contribute surface emission only on the nightside [58, 59], but are too narrow and low in flux to detect at interstellar distance.

iii. Redox Chemistry

Spectrophotometry can detect a sufficient variety of compounds to indicate whether energy yielding reactions in a regenerative cycle would be possible. The TPF should be able to provide this information [60].

iv. Tidal Flexing

Internal heating is a significant source of internal heating in planets due to cyclic variations in gravitational interactions. This can be predicted from factors like mass, orbital characteristics, and proximity to other planets and central stars. Tidally locked planets have lower habitability prospects due to the separation of extreme hot and light conditions. Atmospheric circulation can transfer heat to the dark side, widening the area of habitability [61]. Remote sensing techniques can determine if a planet is within a tidally locked zone.

### 2.4.6. Chemical conditions

Polymeric chemistry is crucial for life, [62] and carbon has desirable chemical properties and molecular bonding for biopolymer formation. It can form covalent bonds with nitrogen, sulfur, phosphorus, and oxygen [63]. Silicon can also form polymers, but they can be unstable over a wide temperature range. Organosilicates are a known component of living systems [54, 64, 65]. Detecting organic compounds, such as organosilicates or silicon polymers, is a positive indicator of the existence of biomolecules. The presence of nitrogen, sulfur, and phosphorus further enhances the probability of organic heteromolecules, which makes the presence of complex chemistry more likely.

### 2.4.7. Liquid water

Liquids in the atmosphere, surface, or beneath the surface are determined by chemistry, pressure, and temperature. Direct imaging can detect clouds, which can suggest airborne liquids. Temperature and pressure values can also suggest liquids on the surface. Direct imaging can detect surface liquids on exoplanets. Techniques such as asynchronous rotation of magnetic fields with planetary rotation, as used to infer the presence of subsurface oceans on icy satellites like Europa [66], may be tricky to apply at a great distance. Geysers, as observed on Enceladus [67], give evidence of

subsurface liquids, but they too may be difficult to detect by direct imaging until telescopes become much more powerful. Indirect inference from data on density, chemical composition, surface temperature, and, if possible, surface pressure may be the best hope for estimating the possibility of subsurface liquids.

## 2.5. Existing Atmospheric Models for Characterization

### 2.5.1. Components of Exoplanet Atmospheres

#### 2.5.1.a. Molecular Detections and Abundances

Planetary atmospheres are primarily composed of molecules, with the relative abundances of different species influenced by the planet's formation, evolution, differentiation, atmospheric circulation, and photochemical processes. In equilibrium conditions, CO and $H_2O$ are the most abundant and spectroscopically active species on most giant exoplanets in solar-like abundances of 1000–2500 K temperatures [68, 69]. $CO_2$ is present in high metallicity environments at these temperatures, but its abundance remains lower than CO for all but the highest metallicities [70]. CH4 and NH3 become more abundant below approximately 1300 K and 700 K, respectively [68]. Various molecules detected by spectroscopy or broadband photometry are reviewed in the following sections:

i. Spectroscopically Resolved Molecules

Exoplanets' atmospheric molecular abundances are most reliably detected and measured through observations that resolve individual lines or the overall shape of molecular bandheads. $H_2$ is the dominant constituent of most exoplanets studied, with transiting planets revealing planet densities fit with significant $H_2$ envelopes [71]. Substantial $H_2$ can also be inferred from the Rayleigh scattering slope of a planet's transmission spectrum [72], as seen in hot Jupiters and Neptune-sized GJ 3470b. $H_2$ also makes itself known via continuum-induced absorption (CIA). CO is abundant in giant, hot exoplanet atmospheres due to its regularly-spaced rovibrational lines, making it easy to detect at high dispersion. $H_2O$ is roughly as abundant as CO in the atmosphere (see Fig. 1) and sculpts their NIR spectra more strongly than CO. Medium- and high-dispersion spectroscopy has detected the species in a growing number of directly imaging planets [73-76] and hot Jupiters [77-79]. CH4 is expected to be less abundant than CO in all but the coolest exoplanets studied to date, and even in cooler planets, disequilibrium processes tend to decrease $CH_4$ abundance in favor of CO. The most convincing spectroscopic detection of $CH_4$ to date is for the directly-imaged planet HR 8799b. At temperatures around 500 K, NH3 becomes increasingly abundant, with evidence in sub-equilibrium abundances in cool brown dwarfs and solivagant planetary-mass objects [80-82]. At warmer temperatures of hot Jupiters, TiO and VO could cause prominent features similar to those seen in M stars [83]. Tentative spectroscopic evidence for TiO was reported in HD 209458b [84], but subsequent high-dispersion spectroscopy shows no evidence of the molecule [85].

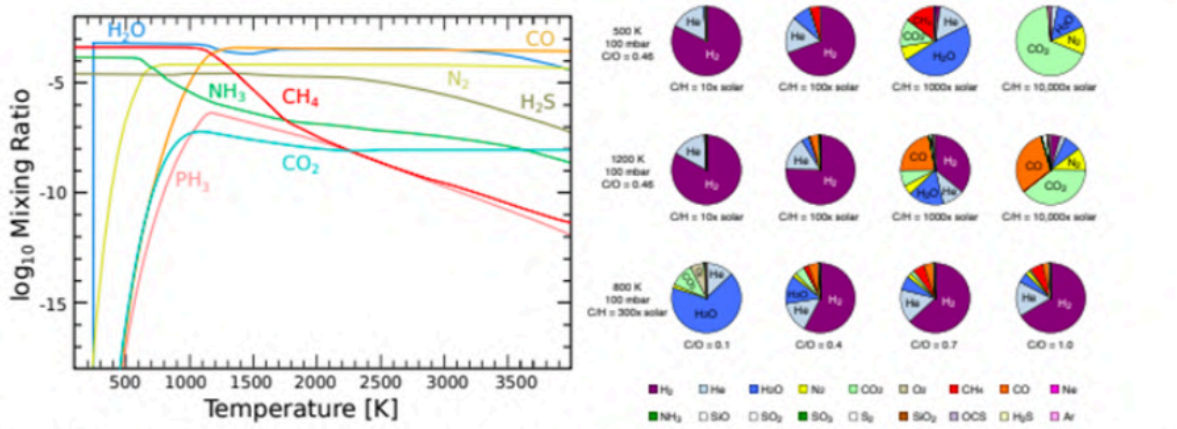


FIG. 1 — Molecular equilibrium abundances: *Left*: vs. temperature in a Solar-metallicity atmosphere at a total pressure of 1 bar; rainout, photochemistry, quenching, etc. are all neglected (adapted from Sharp & Burrows 2007, Miguel & Kaltenegger 2014). $H_2$ would be above the top of the plot. *Right:* For generic hot Neptunes with a range of temperatures, metallicities, and C/O ratios (from Moses et al. 2013).

ii. Molecular Abundances from Broadband Photometry

Broadband data, obtained at multiple epochs, is more susceptible to calibration drifts than spectroscopy, especially when comparing transit measurements when the host star is variable or spotted [86-88]. Despite these challenges, broadband data are easier to acquire than spectroscopy, so photometry has historically preceded dedicated spectroscopic followup. The Spitzer/IRAC camera has observed photometric transits and eclipses of more planets than any other facility, often working in conjunction with ground-based imagers. However, revisions in early Spitzer photometry have led to the suggestion that broadband transit photometry may be less precise than previously claimed [89]. Plans to use these techniques to study habitable super-Earths' atmospheres should be treated with caution [90, 91].

2.5.1.b. Carbon-to-Oxygen Ratios

Carbon and oxygen are the two most common elements in the Sun after H and He [92], and they are expected to form a few dominant molecular species in the planetary atmosphere when in chemical equilibrium. The carbon to oxygen (C/O) ratio of a planet's atmosphere strongly affects the relative abundances of these molecules [93, 94] (see Fig. 1) and may hold clues to the planet's formation and evolution. Exoplanets with a carbon-oxygen (C/O) ratio significantly different from their host star have not been found. Medium-resolution spectroscopy of planets HR 8977b and c shows their atmospheres to be consistent with a solar C/O of approximately 0.65±0.1 [76, 95]. High-dispersion spectroscopy of Jupiter HR 179949b revealed a low-S/N measurement of C/O= 0.5 +0.6 −0.4 [45]. Transiting gas giants also find no unusual C/O ratios. However, additional eclipse measurements [96-98], accounting for a nearby M dwarf binary [97, 99], and independent retrieval analysis demonstrated that existing data were insufficient to justify claims of C/O>1 [100]. New measurements and a reanalysis of old data and atmospheric retrieval have generated a counter-claim that WASP-12b does

show C/O>1 (though this last analysis ignored multiple data points not well-matched by the data) [101].

2.5.1.c. Disequilibrium Chemistry and High Metallicity Atmospheres

The Solar System's atmospheres are not in chemical equilibrium and all exhibit higher metallicity than the Sun. At high altitudes, photochemistry from the Sun's irradiation induces new reactions, such as the formation of $O_3$ (ozone) from $O_2$ in Earth's upper atmosphere [102]. Vigorous internal mixing can "quench" abundances, resulting in CO observed in Jupiter's cold atmosphere. Gas giants in the Solar System become increasingly enriched in heavier elements with decreasing mass. Disequilibrium and elemental composition significantly shape local and exoplanetary atmospheres, with most strongly affecting planets with temperatures above 2000 K [103, 104]. Cooler planets may exhibit disequilibrium conditions, while hotter planets are near equilibrium. The 3000 K WASP-33b is a possible high temperature outlier [105], warranting further studies of this object.

i. In Transiting Planets

Disequilibrium chemistry and high metallicity in exoplanet atmospheres are discussed, particularly in the thermal emission spectrum of Neptune GJ 436b. The planet's high $CO/CH_4$ ratio could be attributed to a high-metallicity atmosphere. JWST eclipse spectroscopy could demonstrate the impact of disequilibrium, high-metallicity, and unusual abundance patterns on GJ 436b and other sub-Jovian planets [106].

ii. In Directly Imaged Planets

Directly imaged planets offer higher-quality data for detailed atmospheric chemistry and disequilibrium studies than transiting systems. These young, hot planets exhibit higher $CO/CH_4$ ratios than expected from equilibrium models and solar abundances [107-110]. However, molecular abundances for these systems are less frequently reported than transiting systems. A more systematic analysis of these planets' atmospheric conditions and molecular abundances would benefit the field [106].

2.5.1.d. Alkalis, Ions, and Exospheres

Hot Jupiters have temperatures up to 3000 K on their day sides, as hot as some M stars, at pressures of ~1 bar. At lower pressures, atmospheric density decreases until local thermodynamic equilibrium is met. In the high-altitude exosphere, temperatures can reach up to ~10,000 K, hot enough to split molecules and partially ionize constituent atoms. Fig. 2 shows theoretical abundance profiles of some of the more common species predicted to exist in these planets' atmospheres [111]. Alkali species, such as sodium, were the first constituents detected in hot Jupiter's atmosphere [112, 113]. Mass loss and high-altitude atomic species have been observed in a growing number of short-period transiting planets using ultraviolet HST transit spectroscopy. Mass loss is understood to result from hydrodynamic Roche lobe overflow of the planet's exosphere,

powered by the extremely high-energy X-ray and FUV flux of the host star. Atmospheric mass loss from lower-mass planets is even less well studied than from hot Jupiters, with only Ly α transit observations of hot Neptune GJ 436b and the ~2000 K sub-Neptune 55 Cnc e [106].

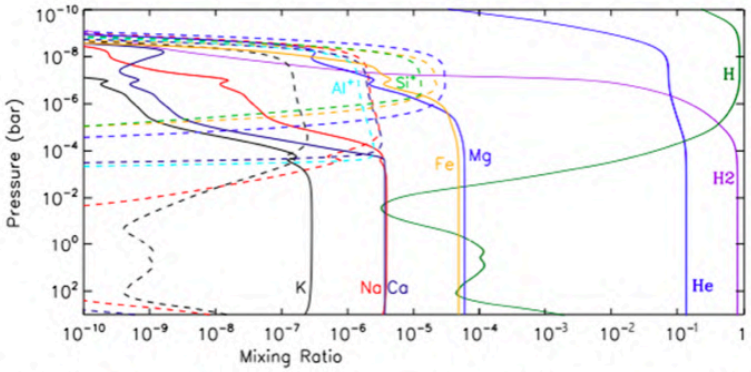


FIG. 2 — Theoretical abundance profiles of atomic and ionized species in the atmosphere of hot Jupiter HD 209458b. Solid lines are neutral species; dashed lines of the same color indicate the corresponding ion. Observations of these species probe mbar-to-μbar levels, much higher than the bar-to-mbar levels probed by thermal emission measurements. Adapted from Lavvas et al. (2014).

### 2.5.2. 1D Atmospheric Models

#### 2.5.2.a. ATMOS 1D

i. Introduction

Clouds are essential in planetary radiative budgets, reflecting incoming star light and absorbing thermal infrared radiation. Their dominant effect depends on factors like cloud type, composition, altitude, surface temperature, and stellar spectrum. Clouds are considered "grey" absorbers due to their wavelength-independent absorption. Some 1-dimensional climate models of early Earth and other planets are cloud-free, adjusting surface albedo to reflect cloud albedo and mean surface temperature [114]. This assumption is widely used in 1D climate models [115-126], which represent the atmosphere in a single, horizontally homogeneous vertical column. The study [127] demonstrates that clouds' effects can be simulated by tuning surface albedo, and mean energy budgets deviate from observations for both shortwave and long-wave radiations. The research uses this methodology to explicitly represent clouds in the Atmos 1D climate model, improving its ability to represent cloud effects in future atmospheric studies.

ii. Overview

The Atmos 1D climate model was utilized to simulate the climates of various rocky planets, including Venus, Earth, Mars, and exoplanets. The model uses correlated-k absorption coefficients from HITRAN 2008 and HITEMP 2010 databases for pressures and temperatures. For Earth simulation, a 1976 US standard atmosphere with modern greenhouse gases was considered. The model has historically been used to simulate planets within the habitable zone [124].

#### 2.5.2.b. Radiative-Convective Climate Model

##### i. Introduction

Scientists have been using computer models to study Earth's climate for the past three decades. This work presents a physical climate model, a one-dimensional time dependent radiative convective climate model (1D RCM), developed at the Oregon Graduate Institute (OGI). This model is commonly used to study the impact of increasing trace gas concentrations, particularly $CO_2$, $CH_4$, $N_2O$, $CC1_3F$, $CC1_2F_2$, and other gases from human activities. The model is compared to other similar RCMs, assessing its sensitivity to perturbations and strengths and weaknesses for other modelling applications [128].

##### ii. Overview

Earth's climate is a complex system involving interactions between the sun, atmosphere, biosphere, cryosphere, hydrosphere, and geosphere. Physical climate models help simulate major features of the climate system and understand processes that produce past, present, and future climates. Two important questions addressed when modeling the Earth's climate are the change in mean global temperatures due to perturbations in the climate system and the mean effect on regional precipitation patterns resulting from climatic perturbations. The OGI 1D RCM fits into the climate modelling hierarchy, including zero-dimensional or 1-box climate models, one-dimensional (1D) climate models, two-dimensional models, and three-dimensional general circulation models (GCMs). It includes 18 atmospheric layers and the Earth's surface, solving for the vertical temperature structure of the Earth-atmosphere system as the primary indicator of climate [128].

### 2.5.3. 3D Atmospheric Models

#### 2.5.3.a. ECHAM 6

ECHAM is a general circulation model (GCM) developed by the Max Planck Institute for Meteorology, a research organisation of the Max Planck Society. It was created by modifying global forecast models developed by ECMWF for climate research. The model was given its name as a combination of its origin (the 'EC' being short for 'ECMWF') and the place of development of its parameterisation package, Hamburg. The model resolves the atmosphere up to 10 hPa (primarily used to study the lower atmosphere), but can be reconfigured to 0.01 hPa for stratosphere and lower mesosphere studies. ECHAM6 is the most advanced version of the ECHAM models. The MPI Earth System Model (MPIESM) is a new version of ECHAM6, including land vegetation model JSBACH, ocean GCM MPIOM, and ocean biogeochemistry model HAMOCC. It has been developed on the basis of ECHAM5 [129, 130], with significant differences in land processes, radiation schemes, surface albedo computation, and

convection triggering conditions. The technical infrastructure has been significantly modified to optimise computational performance on the current DKRZ high-performance computer. JSBACH land vegetation model has been integrated into ECHAM6, including parameterisations for physical aspects such as heat and water storage, photosynthetic activity of plants, carbon allocation and storage in plants and soils, and soil respiration. Reflective forcing in ECHAM6 has been modified, with the SW and LW schemes replaced and the surface albedo scheme improved for sea, sea ice, and snow-covered land. ECHAM6 has been developed for resolutions T63L47, T63L95, and T127L95, with spectral representations associated with Gaussian grids of approximately 1.9 deg and 0.95 deg resolution [131].

2.5.3.b. The STAGGER-Grid

Stellar objects' light provides information about their origin, but accurate interpretation requires models of atmospheric layers at the star's surface. Late-type stars face challenges in theoretical modelling due to convective motions, turbulent flows, and magnetic fields. Accurately accounting for the interaction between radiative and convective energy transport at the optical surface is crucial for accurately representing temperature stratifications in outer layers. The first realistic grids of line-blanketed atmosphere models for late-type stars appeared with the publication of MARCS and ATLAS models. Subsequently, one-dimensional (1D) atmosphere codes, such as PHOENIX and MAFAGS, were developed to model the atmospheres of stars. These models assume hydrostatic equilibrium, flux constancy, and local thermodynamic equilibrium (LTE), commonly employing the mixing-length theory (MLT). They commonly employ the mixing-length theory (MLT), which is characterised by several free parameters, such as the mixing-length lm or equivalently, the parameter $\alpha_{MLT} = l_m/H_P$.

Constructing simple yet realistic 1D models of convection is difficult, especially considering convective overshooting beyond the classical Schwarzschild instability criterion [132, 133]. Semi-empirical models are almost exclusively used for solar atmosphere modelling, inferring temperature stratification from observations. Constructing more realistic models requires going beyond the 1D framework and modelling convection without relying on MLT. For metal-poor late-type stars, it has been shown [134-136] that, the assumption of pure radiative equilibrium in the convectively stable photospheric layers of classical hydrostatic models is generally insufficient. 1D models often overestimate temperatures by up to ~1000 K at very low metallicities, leading to systematic errors in abundance determinations [137-140]. These shortcomings manifest as inconsistencies in the analysis of observed spectra, such as abundance trends with excitation potential of lines (e.g. analysis of NH lines in the very metalpoor star HE1327-2326) [141] and discrepant abundances between atomic and molecular lines involving the same elements. Surface effects point to mistakes in the outer layers of theoretical 1D stellar-structure models [142]. 3D solar models have predicted p-mode excitation rates closer to helioseismic observations [143, 144]. Stellar

radii have been derived for several red giants from interferometric observations, which impact the zero point of the effective temperature scale derived by interferometry. Several 3D magnetohydrodynamics codes have been developed and applied to the modelling of stellar surface convection, such as the Stagger-code, Bifrost-code, CO5BOLD, MURaM, and ANTARES. Most of the available 3D stellar convection codes are highly parallelized, making it feasible to construct grids of 3D convection simulations within a reasonable time-scale [145].

### 2.5.4. Role of Computational Methods in Exoplanet Studies

#### 2.5.4.a. Computational Intelligence in Astronomy

##### i. Introduction

The advancement of technology in observational instruments in astronomy has led to a significant increase in astronomical data, including high-dimensional and multi-modal data. The Digitised Palomar Observatory Sky Survey (DPOSS) [146] generated 3 TB of image data, while the Sloan Digital Sky Survey (SDSS) [147] has reached 40 TB. The Large Synoptic Survey Telescope (LSST) is expected to generate 30 TB of data per observation night, with 100,000 variable objects found every night. The data boom is primarily due to the development of CCD technology, which allows for direct digitisation of astronomical data into electronic documents, improving data collection efficiency [148]. Large astronomical surveys have become the primary means for astronomers to study the universe, presenting new scientific opportunities and challenges. The data-intensive era of astronomy necessitates the focus on automated, efficient, and intelligential techniques to mine large-scale astronomical data for scientific discoveries. Computational intelligence (CI) techniques can help solve complex problems in astronomical data analysis, such as recognising known objects, discovering unknown objects, and searching for rare objects [149].

##### ii. Artificial neural networks in astronomy

Artificial Neural Network (ANN) is a data-driven, self-adaptive computational intelligence technique that approximates general nonlinear functions. It is easy to use and understand, unlike other parametric models. Since its first astronomical application in 1990 [150], ANN has been widely used in tasks such as morphological classification, photometric redshift evaluation, star/galaxy classification, stellar classification, atmospheric parameters estimation, and pulsar candidate identification [149].

##### iii. Fuzzy set theory in astronomy

Fuzzy set theory, developed to describe linguistic expressions in daily life, has been applied in fields like artificial intelligence, pattern recognition, control engineering, decision theory, and expert systems. It imitates human thinking patterns, making it easy

to understand and suitable for realistic problems. Fuzzy methods have been successful in astronomical data analysis since the 1980s, including solar activity prediction [151] and classification tasks.

iv. Evolutionary computation in astronomy

Evolutionary Algorithms, based on Darwinism, are effective in handling complex optimisation problems in astronomy. These algorithms generate a population of individuals, each a solution to a problem. The quality of an individual is measured by its fitness, and their effectiveness is attributed to their ability to handle large amounts of data [152].

2.5.4.b. Data-driven approaches to estimating the habitability of exoplanets

Astronomy has gained significant attention in recent years, particularly in the exploration of exoplanets [153]. These celestial bodies orbiting stars beyond our solar system offer promising insights into the universe's complexities [154]. The advent of space missions and telescopes has flooded the scientific community with vast data, but also presented challenges in analysing this data. This has led to the convergence of astrophysics and data science, with computational models and machine learning techniques revolutionising the field [156]. The confluence of astrophysics and data science, as highlighted by the reviewed literature [153-166], signifies an exciting frontier in scientific research. This intersection opens up a realm of opportunities for the study and exploration of exoplanets, offering new avenues to decipher the mysteries of the universe.

2.5.4.c. Limitations

Exoplanet discoveries have increased significantly due to new telescopes, technological advancements, and increased interest in exoplanet science. Despite the limited number of stars observed in star clusters, there have been several detections of planets in open star clusters, many with orbital parameters unlike those around field stars. As of this work's publication, 34 planets have been observed within 10 Galactic open clusters. The vast diversity of the planetary population is evident in these exoplanets, which display the vast diversity of the planetary population. Understanding the origins of exoplanet systems' orbital properties requires a detailed study of their dynamical histories. Modeling the dynamics of planetary systems in star clusters is a complex problem due to the different timescales involved [167].

# 3. Materials and Methods

## 3.1. Introduction and Overview

The pursuit of this project is set in exoplanet detection and habitability assessment, using data from NASA's retired Kepler Space Telescope. Our primary goal is to apply machine learning techniques to identify potential exoplanets within celestial datasets and to assess their habitability based on a range of astrophysical factors.

The Kepler Space Telescope's database serves as the source of data for our research. We have undertaken an approach using the application of advanced machine learning models such as Random Forest Classifier and K-Nearest Neighbors (KNN) for the accurate classification of these celestial bodies. In addition to detection, our project extends into evaluating the habitability of exoplanets, employing criteria like planetary radius, orbit semi-major axis, stellar surface gravity, and equilibrium temperature.

In this section, we will articulate the steps of our project, from the acquisition of data to its preprocessing, which involved renaming columns for clarity, refining the dataset by removing irrelevant columns, and ensuring data integrity by excluding rows with missing or infinite values. We will also be discussing the software tools and libraries integral to our research.

## 3.2. Software and Libraries

### 3.2.1. Programming environment

Our project is developed within Google Colab, a free cloud service based on Jupyter Notebooks that supports Python programming. Google Colab is particularly advantageous for machine learning and data science projects due to its easy access to powerful computing resources, including GPUs and TPUs, and its seamless integration with Google Drive for data storage and sharing.

### 3.2.2. Libraries and Tools

Our project relies on a selection of specialized Python libraries and tools, each contributing to different aspects of the project:

1. **Pandas and NumPy**: Essential for data manipulation and numerical computing. Pandas provides easy-to-use data structures and data analysis tools, while NumPy supports large, multi-dimensional arrays and matrices along with a broad collection of mathematical functions.
2. **Matplotlib and Seaborn**: These libraries offer versatile plotting capabilities. Matplotlib is used for creating static, interactive, and animated visualizations, and

Seaborn, based on Matplotlib, provides high-level interfaces for drawing attractive and informative statistical graphics.

3. **Scikit-learn**: This library is central to our machine learning tasks. It provides simple and efficient tools for data mining and data analysis, including numerous algorithms for classification, regression, clustering, and model evaluation.
4. **TensorFlow and Keras**: TensorFlow is an end-to-end open-source platform for machine learning, and Keras is a high-level neural networks API running on top of TensorFlow. They are used for building and training our advanced neural network models.
5. **PyTorch**: An open-source machine learning library used for applications such as computer vision and natural language processing, primarily developed by Facebook's AI Research lab.
6. **Scipy**: Used for scientific and technical computing, this library contains modules for optimization, linear algebra, integration, interpolation, special functions, FFT, signal and image processing, and more.
7. **Other Essential Libraries**: Our project also utilizes a range of other libraries, including 'torch' for PyTorch deep learning models, 'imblearn' for handling imbalanced datasets, 'urlretrieve' from 'urllib.request' for data retrieval, and 'pathlib' for path manipulation.
8. **Machine Learning and Data Preprocessing Tools**: We use various sklearn submodules such as 'metrics', 'model_selection', 'preprocessing', 'ensemble', 'neighbors', 'linear_model', 'cluster', 'tree', and 'svm' for different stages of machine learning model development, preprocessing, and evaluation.
9. **Additional Tools and Utilities**: The project also makes use of 'warnings' to manage warnings, 'keras' for deep learning model development, and 'categorical_crossentropy', 'regularizers', 'optimizers' from Keras for model optimization and loss computation.

## 3.3. Data Collection and Processing

### 3.3.1. Data Sources

Our project primarily utilizes data from NASA's Kepler Space Telescope. This retired space observatory, launched by NASA to discover Earth-size planets orbiting other stars, has been a goldmine for exoplanet research. The Kepler mission's publicly available data sets include a vast array of celestial observations, capturing numerous potential exoplanets and various stellar parameters. This data is significant due to its comprehensive coverage of over 150,000 stars in the Milky Way galaxy, leading to the discovery of thousands of exoplanet candidates. By using this repository, we aim to employ machine learning techniques not only to classify these candidates accurately but also to assess their potential habitability.

### 3.3.2. Data Preprocessing

The preprocessing stage is crucial for preparing the raw Kepler data for our analytical models. This phase involved several steps to ensure the data's quality and relevance:
**Data Cleaning and Formatting**: Our initial step involved renaming columns for better clarity and understanding. The original dataset contained concise, sometimes cryptic column names. We mapped these to more descriptive titles to enhance readability and interpretability.

```
df = df.rename(columns={'kepid':'KepID',
'kepoi_name':'KOIName',
'kepler_name':'KeplerName',
'koi_disposition':'ExoplanetArchiveDisposition',
'koi_pdisposition':'DispositionUsingKeplerData',
'koi_score':'DispositionScore',
'koi_fpflag_nt':'NotTransit-LikeFalsePositiveFlag',
'koi_fpflag_ss':'koi_fpflag_ss',
'koi_fpflag_co':'CentroidOffsetFalsePositiveFlag',
'koi_fpflag_ec':'EphemerisMatchIndicatesContaminationFalsePositiveFlag',
'koi_period':'OrbitalPeriod[days',
'koi_period_err1':'OrbitalPeriodUpperUnc.[days',
'koi_period_err2':'OrbitalPeriodLowerUnc.[days',
'koi_time0bk':'TransitEpoch[BKJD',
'koi_time0bk_err1':'TransitEpochUpperUnc.[BKJD',
'koi_time0bk_err2':'TransitEpochLowerUnc.[BKJD',
'koi_impact':'ImpactParamete',
'koi_impact_err1':'ImpactParameterUpperUnc',
'koi_impact_err2':'ImpactParameterLowerUnc',
'koi_duration':'TransitDuration[hrs',
'koi_duration_err1':'TransitDurationUpperUnc.[hrs',
'koi_duration_err2':'TransitDurationLowerUnc.[hrs',
```

For instance:
'kepid' is renamed to 'KepID', which stands for Kepler ID. 'kepoi_name' becomes 'KOIName', representing the Kepler Object of Interest name. ... and so forth for other columns.
After renaming, we display the first few rows of the dataset (df.head()) to quickly inspect the changes and view the data structure.

**Feature Refinement:** We refined the dataset by removing unnecessary columns. This selective exclusion was guided by the relevance of the data to our objectives, focusing on features critical for exoplanet detection and habitability assessment. Such streamlining aids in computational efficiency and clarity.

```
df.drop(columns=['KeplerName','KOIName','EquilibriumTemperatureUpperUnc.[K',
                 'ExoplanetArchiveDisposition','DispositionUsingKeplerData',
                 'NotTransit-LikeFalsePositiveFlag','koi_fpflag_ss','CentroidOffsetFalsePositiveFlag',
                 'EphemerisMatchIndicatesContaminationFalsePositiveFlag','TCEDeliver',
                 'EquilibriumTemperatureLowerUnc.[K'])
```

**Handling Missing Values**: We utilized Pandas functions to identify and eliminate rows with NaN (Not a Number) or infinite values. Ensuring data completeness is vital for the

accuracy of machine learning models. The inplace=True argument ensures that the changes are applied directly to the dataframe without needing to reassign it to a new variable.

```
df.drop(columns=['KeplerName','KOIName','EquilibriumTemperatureUpperUnc.[K',
                 'ExoplanetArchiveDisposition','DispositionUsingKeplerData',
                 'NotTransit-LikeFalsePositiveFlag','koi_fpflag_ss','CentroidOffsetFalsePositiveFlag',
                 'EphemerisMatchIndicatesContaminationFalsePositiveFlag','TCEDeliver',
                 'EquilibriumTemperatureLowerUnc.[K'], inplace=True)
```

**Numerical Validation**: We confirmed that all data points in the dataset were valid numerical values. This step involved removing any non-numeric or infinite values, ensuring that our dataset was primed for the subsequent analytical processes.

```
def clean_dataset(df):
    assert isinstance(df, pd.DataFrame), "df needs to be a pd.DataFrame"
    df.dropna(inplace=True)
    indices_to_keep = ~df.isin([np.nan, np.inf, -np.inf]).any(1)
    return df[indices_to_keep].astype(np.float64)

clean_dataset(df.drop(columns=['KepID']))
```

## 3.4. Methodology

### 3.4.1. Model Training and Evaluation

Each model underwent a training and testing process, where the dataset was split into training and testing sets. The training set was used to train each model, while the testing set was reserved to evaluate the model's performance and generalization capability. We ensured that the data was split in a manner that reflects the real-world distribution of classes, avoiding biases in training or evaluation.

**Data Splitting**: Our next step after data processing involves dividing the dataset into two distinct sets: the training set and the testing set. Typically, we allocate a larger portion of the data (60%) to the training set, with the remaining portion assigned to the testing set. This separation is critical for evaluating the model's performance on unseen data, ensuring it can generalize well beyond the data it was trained on. The train_test_split function from the Scikit-learn library is instrumental in this process, providing a randomized split while maintaining data integrity.

```
[ ] X_train, X_test, y_train, y_test = train_test_split(features, target, random_state=1, test_size=.60)
```

```
# Checking if train test split ran correclty
for dataset in [y_train, y_test]:
    print(round(len(dataset)/len(target), 2))
```

**Model Evaluation:** Post-training, we assess the models' performance using metrics such as accuracy, precision, recall, and F1 score. These metrics provide insights into various aspects of the model's predictions, like its overall correctness (accuracy), its performance in identifying positive cases (precision and recall), and the balance between precision and recall (F1 score). The use of a confusion matrix further aids in visualizing the model's performance in terms of true positives, false positives, true negatives, and false negatives.

```
# Evaluation function

def evaluation(y_true, y_pred):

# Print Accuracy, Recall, F1 Score, and Precision metrics.
    print('Evaluation Metrics:')
    accuracy=accuracy_score(y_test, y_pred)
    precision=precision_score(y_test, y_pred)
    print('Accuracy: ' + str(accuracy_score(y_test, y_pred)))
    print('Recall: ' + str(recall_score(y_test, y_pred)))
    print('F1 Score: ' + str(f1_score(y_test, y_pred)))
    print('Precision: ' + str(precision_score(y_test, y_pred)))

# Print Confusion Matrix
    print('\nConfusion Matrix:')
    print(' TN,  FP, FN, TP')
    print(confusion_matrix(y_true, y_pred).ravel())
    cm=confusion_matrix(y_true,y_pred)
    sns.heatmap(cm, annot=True, fmt='d', cmap='Blues', cbar=True)

    return accuracy, precision

# Function Prints best parameters for GridSearchCV
def print_results(results):
    print('Best Parameters: {}\n'.format(results.best_params_))
```

### 3.4.2. Detection of Exoplanets

To identify potential exoplanets within the dataset obtained from the Kepler Space Telescope, we employed a variety of machine learning models.

**Random Forest Classifier**: Known for its high accuracy, robustness, and ability to handle large datasets with numerous variables, the Random Forest algorithm was a natural choice. By constructing multiple decision trees during training and outputting the class that is the mode of the classes of individual trees, it reduces overfitting risks and offers a more reliable prediction.

```
# Instantiate model
forest1 = RandomForestClassifier(n_estimators=100, criterion='gini')
# Fitting Model to the train set
forest1.fit(X_train, y_train)
# Predicting on the test set
y_pred = forest1.predict(X_test)

# Evaluating model
af,pf=evaluation(y_test, y_pred)
```

**K-Nearest Neighbors (KNN)**: This model was selected for its simplicity and effectiveness in classification problems. KNN works by finding the nearest data points in the training set to a given data point in the test set and predicting the label based on these neighbors. It's particularly useful for its ability to adapt as we collect more data.

```
knn = KNeighborsClassifier(leaf_size=8, metric='manhattan',weights='uniform')

# Fitting Model to the train set
knn.fit(X_train, y_train)

# Predicting on the test set
y_pred = knn.predict(X_test)

# Evaluating model
ak,pk=evaluation(y_test, y_pred)
```

**Logistic Regression**: As a statistical model that predicts the probability of a binary outcome, logistic regression was utilized for its efficiency and the interpretability of its results. It's beneficial for understanding the influence of several independent variables on a binary outcome.

```
# Logistic Regression Model
lr = LogisticRegression(C=100, max_iter=200, class_weight='balanced')

# Fitting Model to the train set
lr.fit(X_train, y_train)

# Predicting on the test set
y_pred = lr.predict(X_test)

# Evaluating model
alr,plr=evaluation(y_test, y_pred)
```

**Decision Tree Classifier:** Decision Trees were employed due to their intuitive nature and ease of interpretation. These models mimic human decision-making processes, making them straightforward to understand and explain. They are particularly useful for binary classification tasks like exoplanet detection.

```
tree = DecisionTreeClassifier()

# Fitting Model to the train set
tree.fit(X_train, y_train)

# Predicting on the test set
y_pred = tree.predict(X_test)

# Evaluating model
at,pt=evaluation(y_test, y_pred)
```

### 3.4.3. Habitability Analysis

The habitability analysis of exoplanets forms a crucial part of our research, aiming to assess the potential of these celestial bodies to support life as we understand it. This assessment is grounded in the calculation of a habitability score, a numerical representation derived from a set of astrophysical criteria considered essential for life.

**Habitability Score Calculation**

The habitability score is calculated through a function that evaluates each exoplanet against specific criteria, with each criterion contributing points to the overall score. This scoring mechanism enables a quantifiable assessment of each exoplanet's potential to be habitable.

**Key Criteria for Scoring:**

1. Planetary Radius: We considered planets with a radius between 0.8 and 1.5 times that of Earth's. This range is indicative of planets that are likely to be rocky and thus capable of sustaining an atmosphere, a fundamental requirement for life.
2. Orbit Semi-Major Axis (Habitable Zone Check): The semi-major axis of an exoplanet's orbit was evaluated against the habitable zone range, which depends on the host star's temperature. The habitable zone, often referred to as the "Goldilocks zone", is the range where conditions might be just right to allow liquid water, a critical ingredient for life.
3. Stellar Surface Gravity: The surface gravity of the star influences the exoplanet's climate and atmospheric retention. We considered a range that aligns with known habitable conditions, specifically 4.0 to 4.9 in log10(cm/s²).
4. Equilibrium Temperature: A temperature range of 273K to 373K was chosen, representing the range in which water can exist in liquid form.

5. Planetary Density/Type of Planet: The density of the planet helps distinguish between rocky planets, gas giants, and mini-Neptunes, with rocky planets being more likely to be habitable.
6. Radiative Flux/Insolation: This criterion assesses whether the planet receives a sufficient amount of stellar energy (insolation) to support life, considering the star's temperature and distance.
7. Eccentricity: Stable, nearly circular orbits (eccentricity <= 0.2) are favored as they are more likely to support stable climatic conditions.
8. Obliquity: The axial tilt of the planet affects its climate and seasonality. A tilt within 45 degrees is considered potentially conducive to stable seasons.

```python
def habitability_score(exoplanet):
    import math
    score = 0

    # Planetary radius
    min_planetary_radius = 0.8  #Minimum radius as a factor of Earth's radius
    max_planetary_radius = 1.5  #Maximum radius as a factor of Earth's radius
    #Assuming 'PlanetaryRadius[Earthradii]' is the column with radius data relative to Earth's radius
    if min_planetary_radius <= exoplanet['PlanetaryRadius[Earthradii']] <= max_planetary_radius:
      score += 1

    # Orbit sem-major axis
    #helper function to check if the exoplanet is in the habitable zone depending on the host star type
    def is_in_habitable_zone(stellar_temp, semi_major_axis):
        if 0.1 <= semi_major_axis <= 5:
            return 1
        else:
            return 0

       #checking if exoplanet is in the habitable zone
    if is_in_habitable_zone(exoplanet['StellarEffectiveTemperature[K']], exoplanet['koi_sma']):
        score += 1

    # Stellar surface gravity
    if 4.0 <= exoplanet['StellarSurfaceGravity[log10(cm/s**2)']] <= 4.9:
        score += 1

    # Equilibrium temperature
    if 273 <= exoplanet['EquilibriumTemperature[K']] <= 373:
        score += 1

    #Type of planet (Planetary density)
    if exoplanet['PlanetaryRadius[Earthradii']]<=1.5:
      score +=1
    elif 1.5<exoplanet['PlanetaryRadius[Earthradii']]<=2.5:
      score +=0.5

    # Radiative flux/insolation/HZ
    fmax=(5.670374419*math.pow(10,-8)*math.pow(exoplanet['StellarEffectiveTemperature[K']],4))/(4*math.pi*(exoplanet['koi_dor']*exoplanet['koi_srad']))
    if 67 <= exoplanet['InsolationFlux[Earthflux']] <= fmax:
        score += 1

    #Eccentricity
    if exoplanet['koi_eccen'] <= 0.2:
        score += 1

    # Obliquity
    if (90-exoplanet['koi_incl']) <= 45:
        score += 1

    return score
```

**Rationale Behind the Chosen Parameters**

The parameters for habitability assessment were chosen based on current astrobiological understanding and research on what makes a planet potentially habitable. These parameters collectively contribute to a holistic evaluation of an exoplanet's environment, factoring in both planetary and stellar characteristics that are believed to be crucial for supporting life.

**Visualizing Habitability Score**

To effectively communicate the results of our habitability analysis, we employed bar chart visualizations.

Bar Chart for Habitability Scores: We created a bar chart to display the frequency of each habitability score obtained by the exoplanets. This chart allows us to assess the number of exoplanets that meet various levels of our defined habitability criteria, highlighting those with scores that suggest a higher likelihood of being habitable.

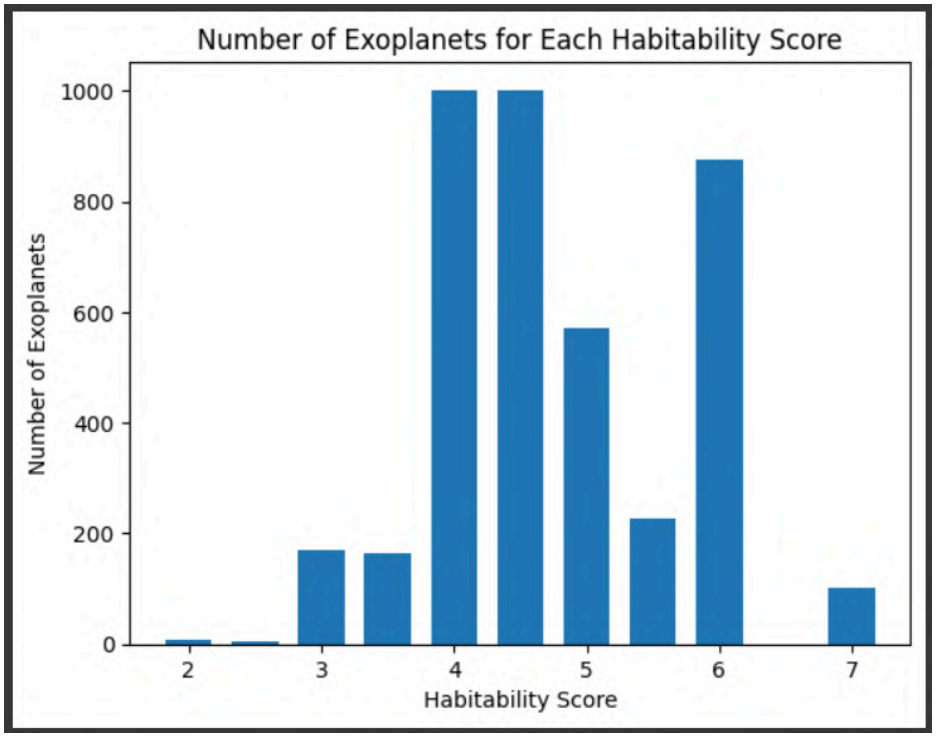


Bar charts for individual conditions: Additionally, we plotted individual habitability conditions to understand better how exoplanets fared against each specific criterion. For each condition, a bar chart was created to show the number of exoplanets falling within and outside the habitable range defined for that particular condition. These charts offer detailed insights into specific areas where exoplanets meet or fail the habitability criteria, aiding in a more nuanced understanding of their potential to support life.

## Planetary Radius

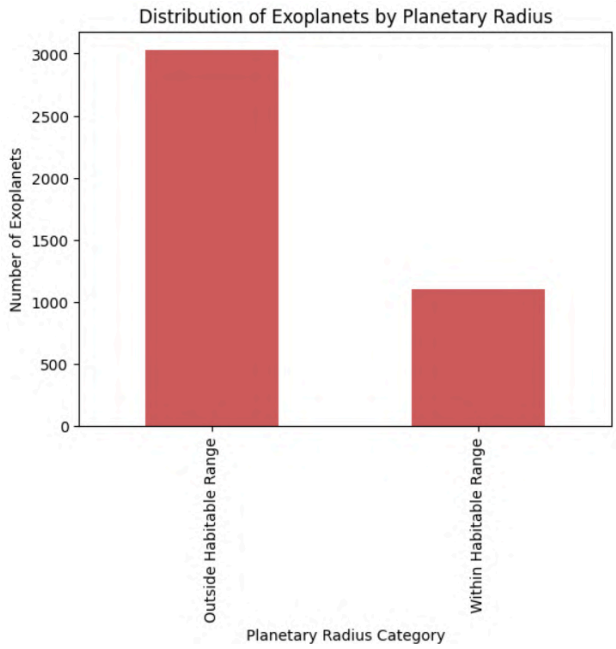


## Orbit Semi-Major Axis

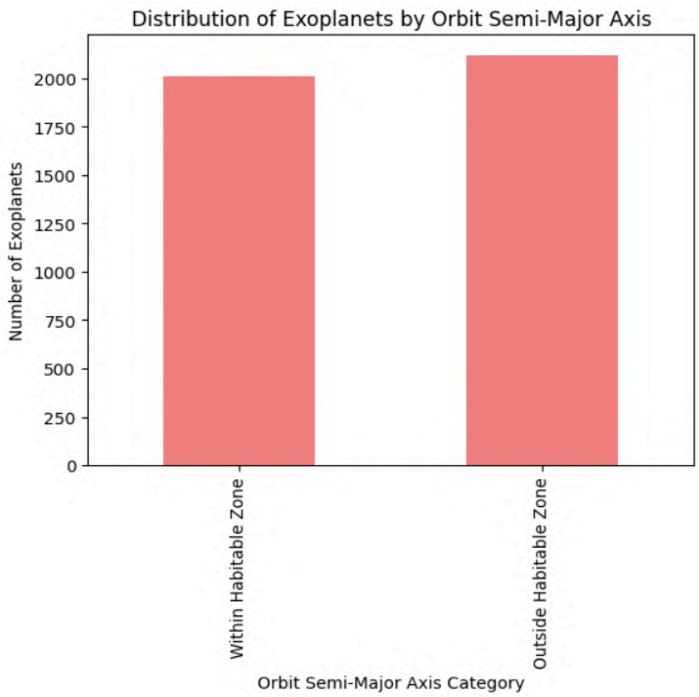


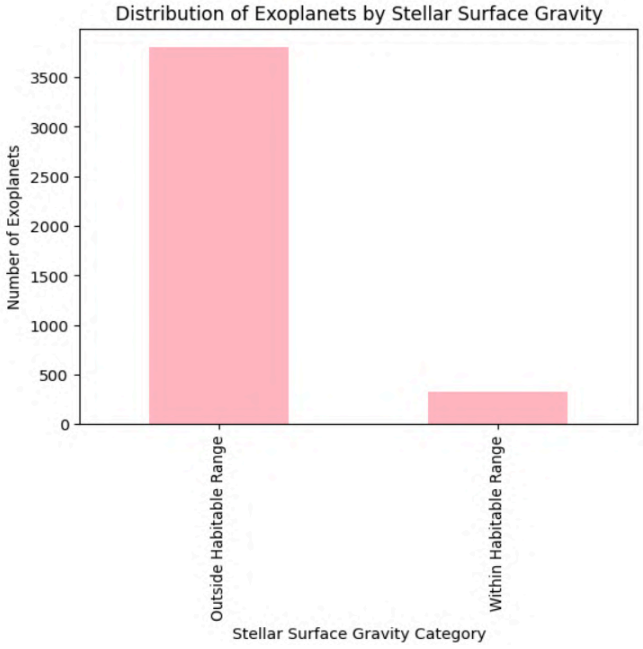


## Stellar Surface Gravity

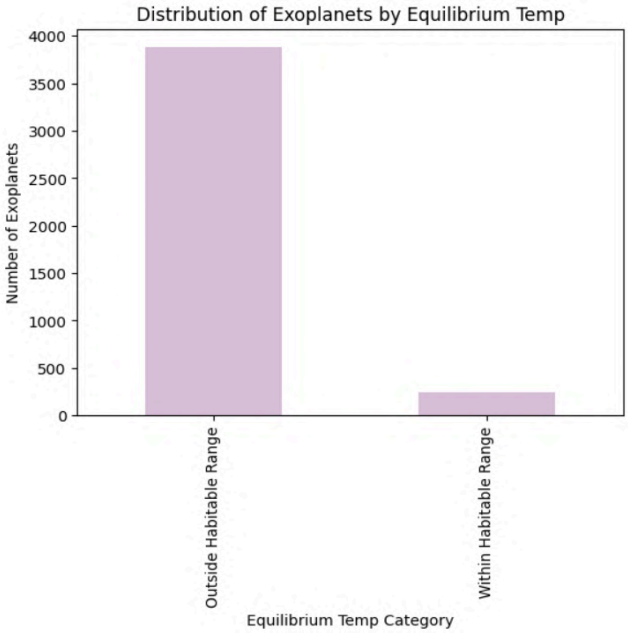


## Temperature

## Equilibrium

## Planetary Density

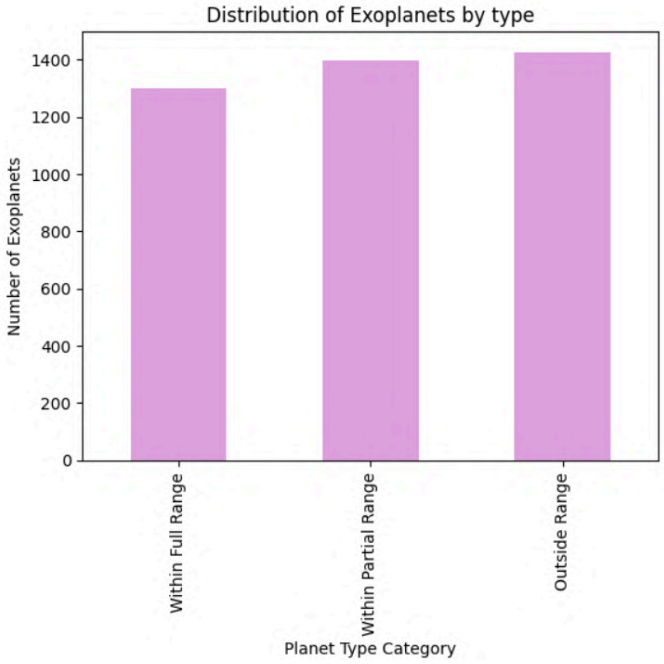


## Radiative Flux

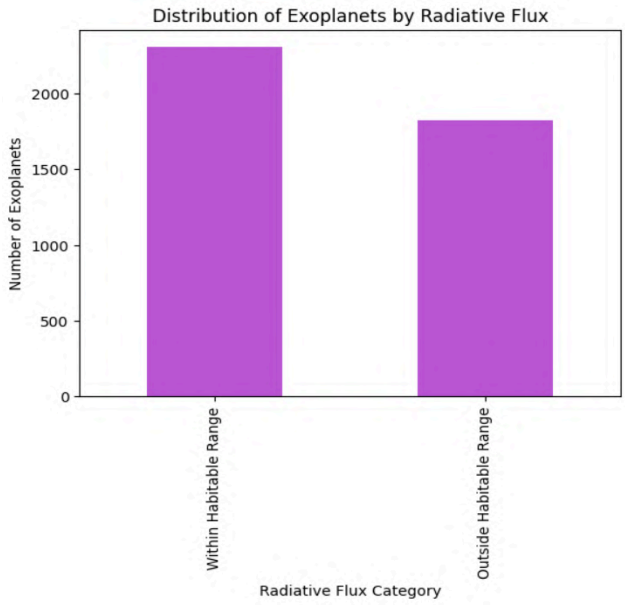


## Eccentricity

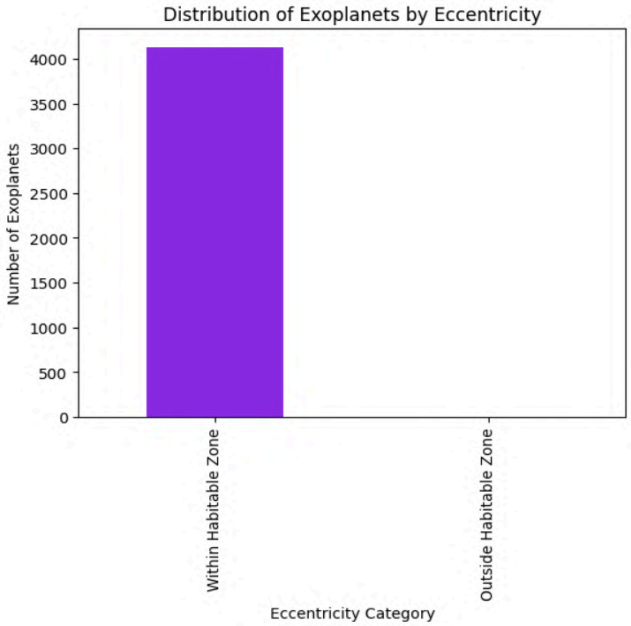


## Obliquity

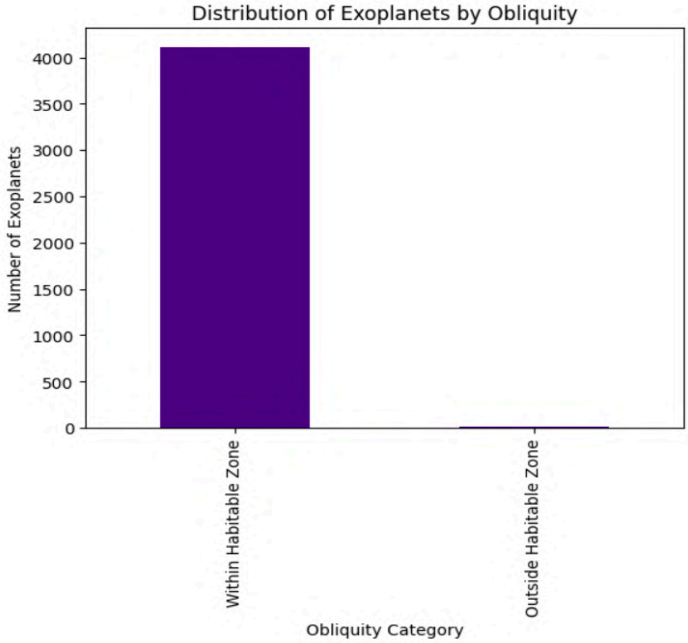

## 3.5. User Input and Interactive Features

Our project integrates interactive features that enable users to input specific parameters and receive immediate predictions or analyses regarding exoplanet detection and habitability assessment. This user-centric approach enhances the application's educational and research value.

### 3.5.1. Exoplanet Detection Interactive Features

- Function Overview: The exoplanetprediction function is an interactive feature allowing users to input key characteristics of a celestial object. The function then utilizes the trained Random Forest model to predict whether the object is an exoplanet.
- User Input Mechanism: The function prompts the user to enter values for various parameters like orbital period, planetary radius, stellar temperature, etc. These inputs are crucial for the model to make accurate predictions.
- Data Handling: The entered values are structured into a pandas DataFrame, mirroring the format used during model training.
- Model Interaction: The user-provided data is fed into the Random Forest model, which then classifies the object as an exoplanet or not based on learned patterns.
- Output Presentation: The function outputs a clear statement, informing the user whether the celestial object fits the criteria of being an exoplanet, enhancing the interactivity and utility of the application.

```
def exoplanetprediction(iv):
  #defining the feature names for which we'll take inputs
  input_features = [
    'DispositionScore', 'OrbitalPeriod[days', 'TransitEpoch[BKJD', 'ImpactParamete',
    'TransitDuration[hrs', 'TransitDepth[ppm', 'PlanetaryRadius[Earthradii',
    'EquilibriumTemperature[K', 'InsolationFlux[Earthflux', 'TransitSignal-to-Nois',
    'TCEPlanetNumbe', 'StellarEffectiveTemperature[K', 'StellarSurfaceGravity[log10(cm/s**2)',
    'StellarRadius[Solarradii', 'RA[decimaldegrees', 'Dec[decimaldegrees', 'Kepler-band[mag]'
  ]

  #setting default values (0) for other features
  default_features = [
    'OrbitalPeriodUpperUnc.[days', 'OrbitalPeriodLowerUnc.[days', 'TransitEpochUpperUnc.[BKJD',
    'TransitEpochLowerUnc.[BKJD', 'ImpactParameterUpperUnc', 'ImpactParameterLowerUnc',
    'TransitDurationUpperUnc.[hrs', 'TransitDurationLowerUnc.[hrs', 'TransitDepthUpperUnc.[ppm',
    'TransitDepthLowerUnc.[ppm', 'PlanetaryRadiusUpperUnc.[Earthradii', 'PlanetaryRadiusLowerUnc.[Earthradii',
    'InsolationFluxUpperUnc.[Earthflux', 'InsolationFluxLowerUnc.[Earthflux', 'StellarEffectiveTemperatureUpperUnc.[K',
    'StellarEffectiveTemperatureLowerUnc.[K', 'StellarSurfaceGravityUpperUnc.[log10(cm/s**2)',
    'StellarSurfaceGravityLowerUnc.[log10(cm/s**2)', 'StellarRadiusUpperUnc.[Solarradii',
    'StellarRadiusLowerUnc.[Solarradii'
  ]


  allfeatures=['DispositionScore', 'OrbitalPeriod[days',
       'OrbitalPeriodUpperUnc.[days', 'OrbitalPeriodLowerUnc.[days',
       'TransitEpoch[BKJD', 'TransitEpochUpperUnc.[BKJD',
       'TransitEpochLowerUnc.[BKJD', 'ImpactParamete',
       'ImpactParameterUpperUnc', 'ImpactParameterLowerUnc',
       'TransitDuration[hrs', 'TransitDurationUpperUnc.[hrs',
       'TransitDurationLowerUnc.[hrs', 'TransitDepth[ppm',
       'TransitDepthUpperUnc.[ppm', 'TransitDepthLowerUnc.[ppm',
       'PlanetaryRadius[Earthradii', 'PlanetaryRadiusUpperUnc.[Earthradii',
```

```
'TransitDurationLowerUnc.[hrs', 'TransitDepth[ppm',
'TransitDepthUpperUnc.[ppm', 'TransitDepthLowerUnc.[ppm',
'PlanetaryRadius[Earthradii', 'PlanetaryRadiusUpperUnc.[Earthradii',
'PlanetaryRadiusLowerUnc.[Earthradii', 'EquilibriumTemperature[K',
'InsolationFlux[Earthflux', 'InsolationFluxUpperUnc.[Earthflux',
'InsolationFluxLowerUnc.[Earthflux', 'TransitSignal-to-Nois',
'TCEPlanetNumbe', 'StellarEffectiveTemperature[K',
'StellarEffectiveTemperatureUpperUnc.[K',
'StellarEffectiveTemperatureLowerUnc.[K',
'StellarSurfaceGravity[log10(cm/s**2)',
'StellarSurfaceGravityUpperUnc.[log10(cm/s**2)',
'StellarSurfaceGravityLowerUnc.[log10(cm/s**2)',
'StellarRadius[Solarradii', 'StellarRadiusUpperUnc.[Solarradii',
'StellarRadiusLowerUnc.[Solarradii', 'RA[decimaldegrees',
'Dec[decimaldegrees', 'Kepler-band[mag]']

input_data = {}
c=0
for feature in allfeatures:
  if feature in default_features:
      input_data[feature] = [0]
  else:
    if len(iv)==0:
    #taking inputs for each feature
      value = float(input(f"{feature}: "))
      input_data[feature] = [value]
    else:
      if len(iv)==17:
        value = float(iv[c])
        input_data[feature] = [value]
        c+=1
```

```
#converting the input data into a DataFrame
input_df = pd.DataFrame(input_data)

#making a prediction using the trained Forest model
predicted_label = forest1.predict(input_df)

#output the prediction result
if predicted_label[0] == 1:
    print("The celestial object is an exoplanet.")
else:
    print("The celestial object is not an exoplanet.")
```

### 3.5.2. Habitability Assessment Interactive Function

- Function Purpose: The habitabilityprediction function lets users input data for a potential exoplanet candidate. The function evaluates the habitability score based on predefined habitability criteria.

- Input Flexibility: Users can either input data manually or provide a pre-compiled list of parameters. The function accommodates both methods, offering versatility in data entry.
- Data Conversion and Analysis: Inputs are converted into a DataFrame and processed through the habitability scoring function, which quantitatively assesses the exoplanet's potential for habitability.
- Habitability Score Display: The final output is a percentage score that indicates the likelihood of the exoplanet being habitable, based on the entered parameters. This score is a valuable tool for both educational purposes and preliminary habitability assessment.

```
def habitabilityprediction(inputdata):
  if len(inputdata)==0:
    #Taking inputs
    print("Enter the details of the exoplanet candidate:")
    planetary_radius = float(input("Planetary Radius (in Earth radii): "))
    orbit_semi_major_axis = float(input("Orbit Semi-Major Axis (in AU): "))
    stellar_surface_gravity = float(input("Stellar Surface Gravity (log10(cm/s^2)): "))
    equilibrium_temperature = float(input("Equilibrium Temperature (in K): "))
    planetary_density = float(input("Planetary Density (Type of Planet, in Earth radii): "))
    radiative_flux = float(input("Radiative Flux (Earth flux): "))
    eccentricity = float(input("Eccentricity: "))
    obliquity = 90-float(input("Obliquity (degrees): "))
    koi_dor = float(input("Distance to Star (AU): "))
    koi_srad = float(input("Stellar Radius (Solar radii): "))
    stellartemp=float(input("Stellar Effective Temperature (in K):"))
  else:
    planetary_radius = float(inputdata[0])
    orbit_semi_major_axis = float(inputdata[1])
    stellar_surface_gravity = float(inputdata[2])
    equilibrium_temperature = float(inputdata[3])
    planetary_density = float(inputdata[4])
    radiative_flux = float(inputdata[5])
    eccentricity = float(inputdata[6])
    obliquity = 90-float(inputdata[7])
    koi_dor = float(inputdata[8])
    koi_srad = float(inputdata[9])
    stellartemp=float(inputdata[10])
  #creating a dataframe with the given exoplanet candidate values
  data = {
    'PlanetaryRadius[Earthradii': [planetary_radius],
    'koi_sma': [orbit_semi_major_axis],
    'StellarSurfaceGravity[log10(cm/s**2)': [stellar_surface_gravity],
```

```
  stellar_surface_gravity = float(inputdata[2])
  equilibrium_temperature = float(inputdata[3])
  planetary_density = float(inputdata[4])
  radiative_flux = float(inputdata[5])
  eccentricity = float(inputdata[6])
  obliquity = 90-float(inputdata[7])
  koi_dor = float(inputdata[8])
  koi_srad = float(inputdata[9])
  stellartemp=float(inputdata[10])
#creating a dataframe with the given exoplanet candidate values
data = {
  'PlanetaryRadius[Earthradii': [planetary_radius],
  'koi_sma': [orbit_semi_major_axis],
  'StellarSurfaceGravity[log10(cm/s**2)': [stellar_surface_gravity],
  'EquilibriumTemperature[K': [equilibrium_temperature],
  'PlanetaryDensity': [planetary_density],
  'InsolationFlux[Earthflux': [radiative_flux],
  'koi_eccen': [eccentricity],
  'koi_incl': [obliquity],  #converting obliquity to inclination
  'koi_dor': [koi_dor],
  'koi_srad': [koi_srad],
  'StellarEffectiveTemperature[K':[stellartemp]
}
candidate_df = pd.DataFrame(data)

#calculating the habitability score
candidate_df['HabitabilityScore'] = candidate_df.apply(habitability_score, axis=1)
print(f"The exoplanet has a {int(100*candidate_df['HabitabilityScore'].iloc[0]/8)}% potential of being habitable.")
```

The integration of these interactive features not only serves to engage users but also provides a practical application of theoretical concepts.

# 4. Hypothesized Results

## 4.1 Exoplanet Detection

For exoplanet detection, we divided the data into x_train, x_test, y_train, and y_test, using 40% for training and 60% for testing. Then, we tested four models and obtained the highest accuracy (~96%) in the Random Forest Classifier.

### 4.1.1 Logistic Regression Model

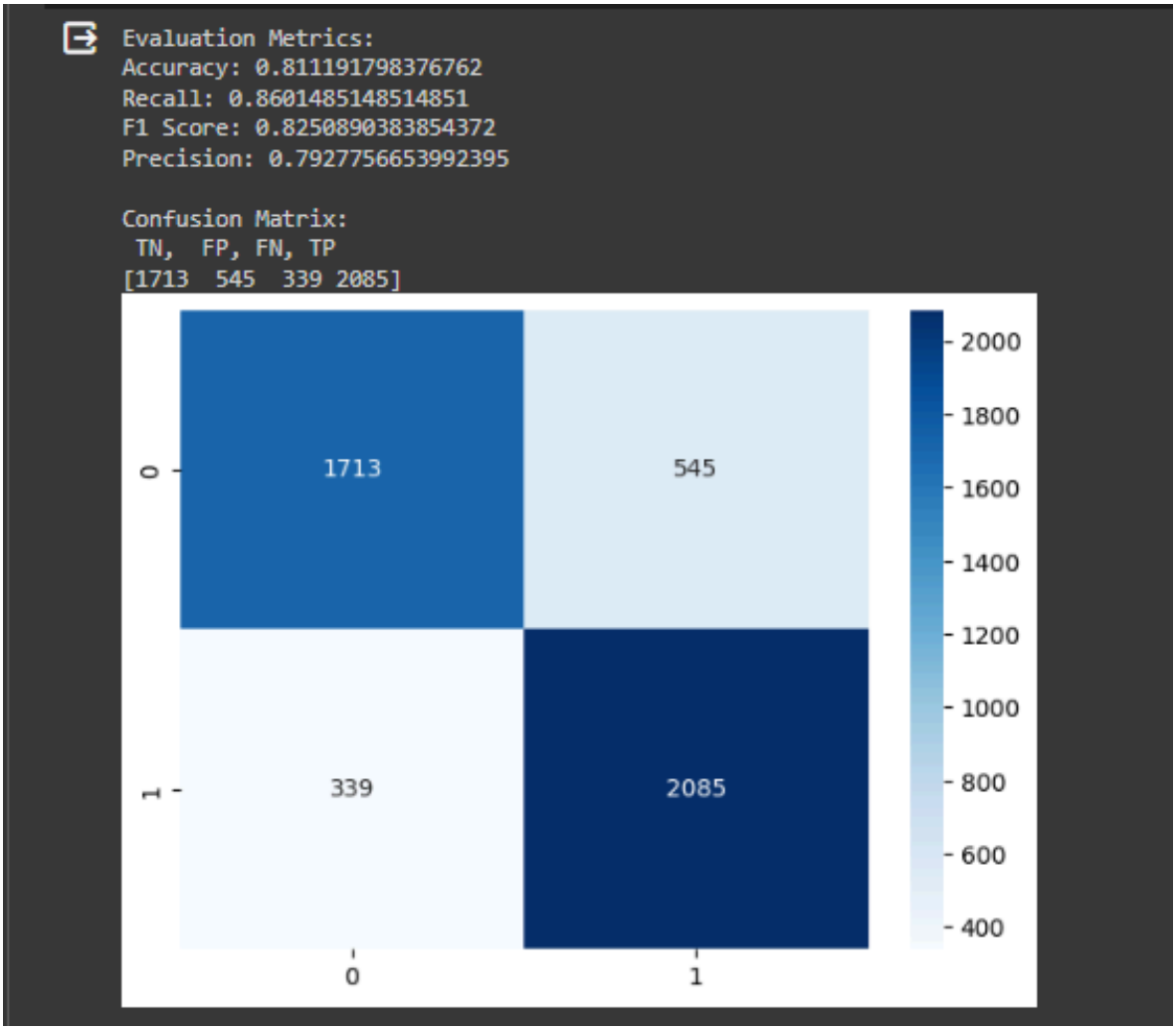

### 4.1.2 KNN Model

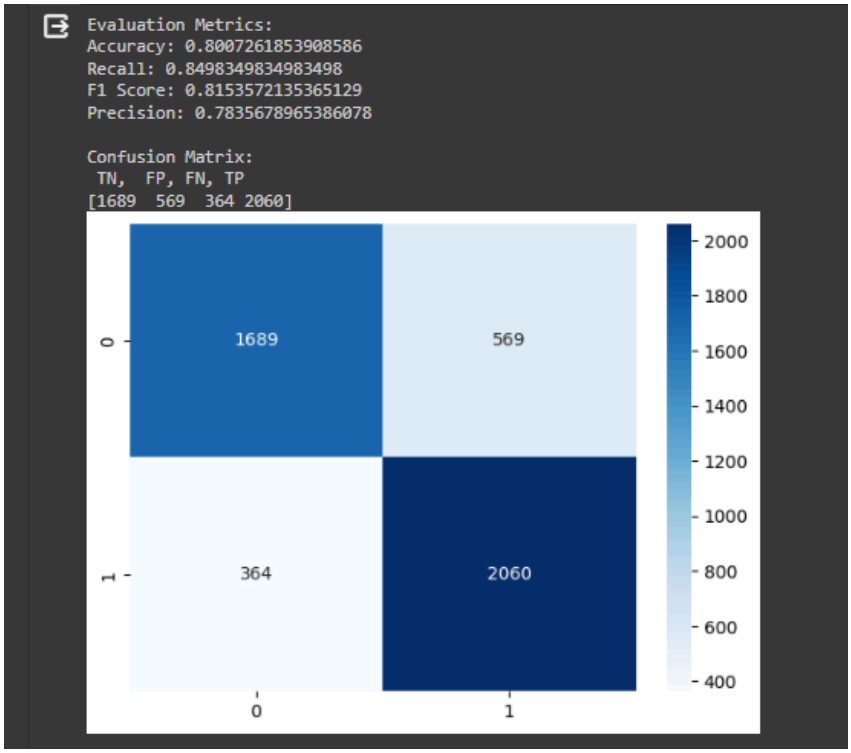


### 4.1.3 Decision Tree Classifier

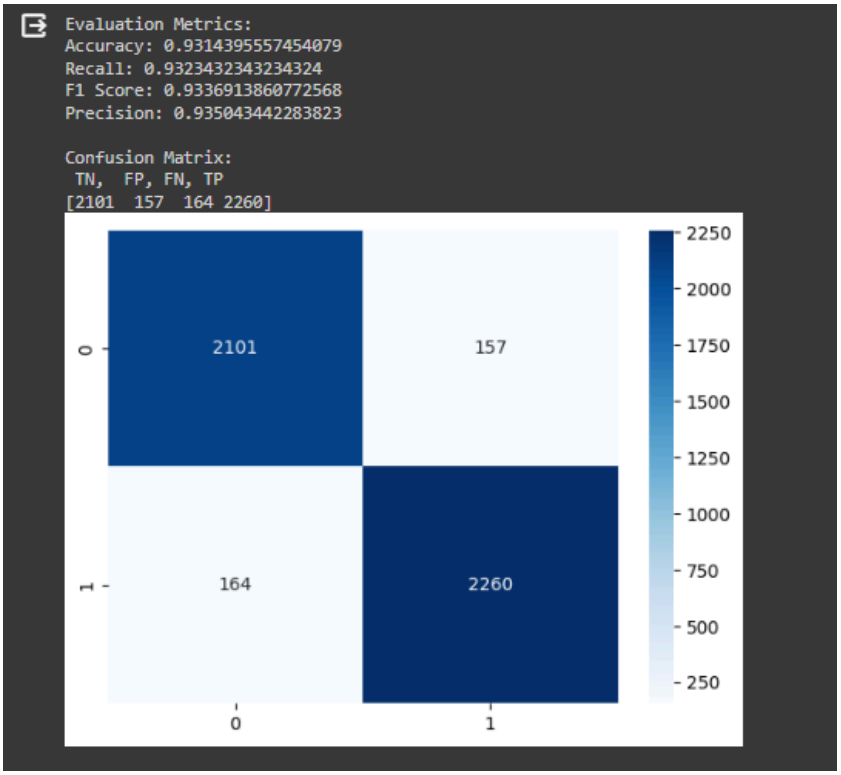

### 4.1.4 Random Forest Classifier

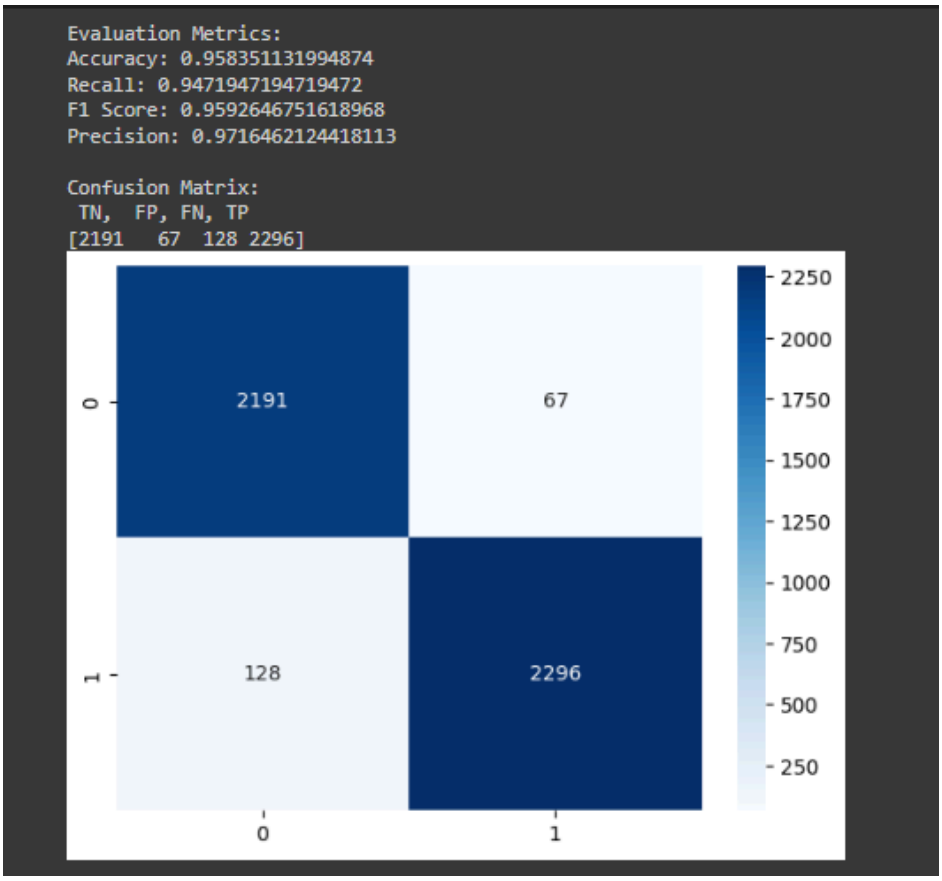


The random forest classifier gave an accuracy of ~96% and a precision of 97%. There were 2296 true positives, 2191 true negatives, 128 false negatives, and 67 false positives. Hence, the error percentage was only 4.4%.

### 4.1.5 Total Exoplanets Found

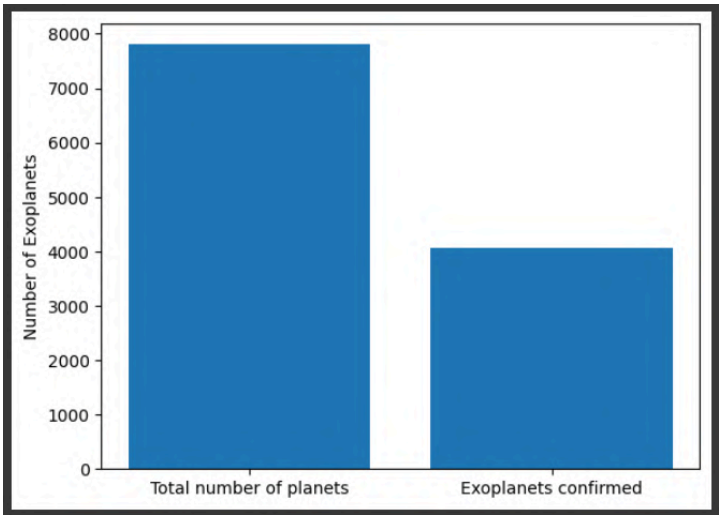


Out of the 7803 celestial objects with appropriate data available, 4068 exoplanets were detected.

## 4.2 Comparison of the various models

The highest accuracy and precision were obtained in the Random Forest Classifier model.

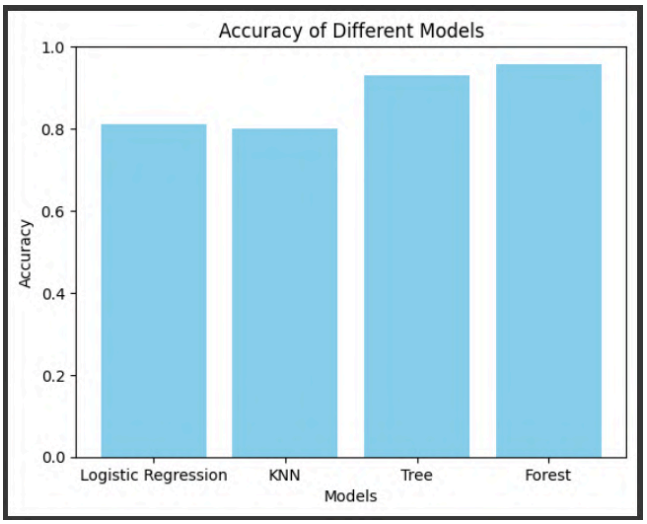


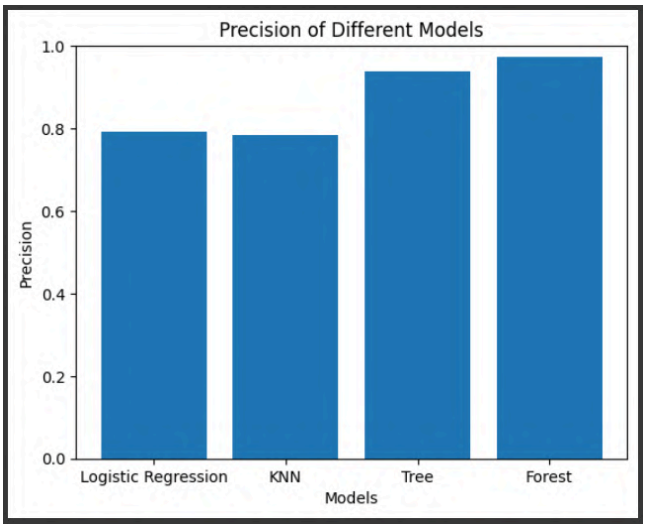


## 4.3 Exoplanet Habitability Potential

According to our model developed for exoplanet habitability potential, every detected exoplanet is analyzed and given a score between 0 to 8, depending on its characteristics like the equilibrium temperature, orbit semi-major axis, obliquity, etc. Then, that score is converted to a percentage to determine the potential for habitability.

### 4.3.1 Obtained Results for Habitability Potential (between 0-8)

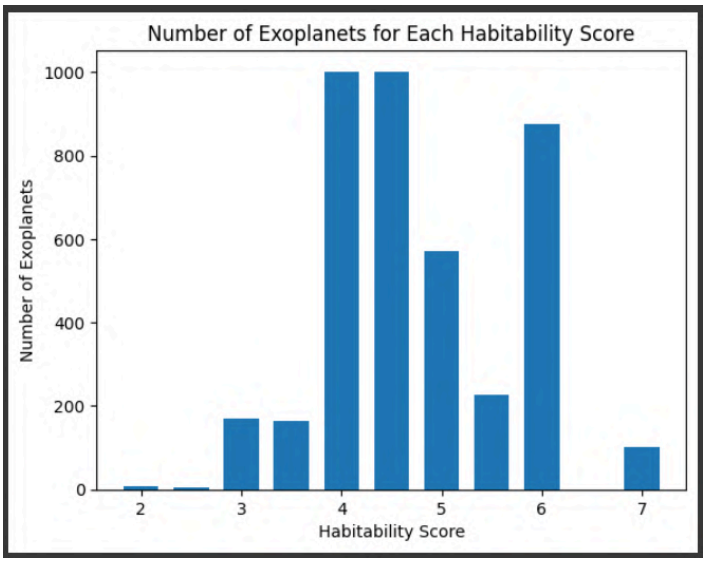

Here, it is important to note that liquid water is an essential condition required but since the temperature largely differs on various exoplanets and may even cause ice to exist underneath the surface, we have not removed exoplanets without a temperature between 273K to 373K. Moreover, no exoplanet has a perfect score of 8, because till now no habitable exoplanet satisfying all conditions of life has been found.

### 4.3.2 Using AI for Score Prediction

We again divided the dataset into x_train, x_test, y_train, and y_test, with 40% for training and 60% for testing. We texted with two models, KNN and Random Forest Classifier.

### 4.3.3 KNN Model

```
KNN Model Evaluation:
Accuracy: 0.53

Confusion Matrix:
 [[  3   1   2   0   0   0]
 [  5  72  70  27  32   0]
 [  0  36 898  90 162   2]
 [  1  36 177 207  74  13]
 [  0  15 320  36 133   0]
 [  0   0  13  42   6   3]]

Classification Report:
              precision    recall  f1-score   support

           2       0.33      0.50      0.40         6
           3       0.45      0.35      0.39       206
           4       0.61      0.76      0.67      1188
           5       0.51      0.41      0.45       508
           6       0.33      0.26      0.29       504
           7       0.17      0.05      0.07        64

    accuracy                           0.53      2476
   macro avg       0.40      0.39      0.38      2476
weighted avg       0.51      0.53      0.51      2476
```

The accuracy was only 53% in this case.

### 4.3.4 Random Forest Classifier

```
Random Forest Model Evaluation:
Accuracy: 0.98

Confusion Matrix:
 [[   2    3    1    0    0    0]
 [   1  195    9    0    1    0]
 [   0    1 1181    6    0    0]
 [   0    0   11  487   10    0]
 [   0    0    0    2  499    3]
 [   0    0    0    1    6   57]]

Classification Report:
              precision    recall  f1-score   support

           2       0.67      0.33      0.44         6
           3       0.98      0.95      0.96       206
           4       0.98      0.99      0.99      1188
           5       0.98      0.96      0.97       508
           6       0.97      0.99      0.98       504
           7       0.95      0.89      0.92        64

    accuracy                           0.98      2476
   macro avg       0.92      0.85      0.88      2476
weighted avg       0.98      0.98      0.98      2476
```

An accuracy of 98% was obtained here.

### 4.3.5 Comparison of the Models

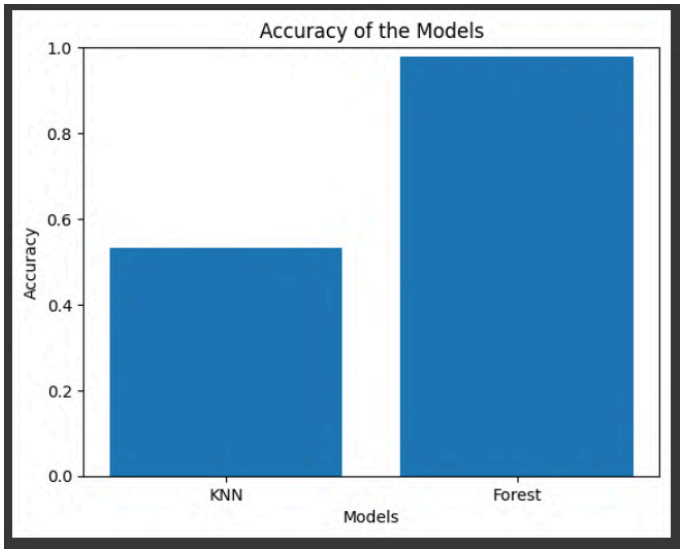


Hence, for both exoplanet detection and habitability potential, the random forest classifier resulted in the highest accuracy.

## 4.4 Exoplanet Detection Using User Input

The Random Forest Classifier method was then used to predict exoplanets for user-input celestial objects too. The function was tested out for existing case studies like Kepler-12 b and K07622.

CASE STUDIES

Here we will check how accurate our detection model is by passing the variables of some already identified and confirmed exoplanet and some non-exoplanets. Our model should print a statement that says, "The celestial object is an exoplanet." if we pass an exoplanet, otherwise it will print "The celestial object is not an exoplanet."

Kepler-12b

```
[113] #A confirmed exoplanet
      kepler12b=[0.76, 4.43, 171, 0.069, 4.69, 16387.6, 18.05, 1338, 757.65, 3535.6, 1, 5953, 4.175, 1.415, 286.24, 50.04, 13.438]
      exoplanetprediction(kepler12b)

      The celestial object is an exoplanet.
```

Kepler-441 b

```
[114] #A confirmed exoplanet in the Habitable Zone
      kepler441b=[0.975, 207.24, 213.03, 0.21, 6.159, 809.2, 1.56, 189, 0.3, 13.2, 1, 4339, 4.711, 0.553, 284.56, 49.01, 15.14]
      exoplanetprediction(kepler441b)

      The celestial object is an exoplanet.
```

K07622

```
[115] #A confirmed non-exoplanet
      k07622=[0, 36.26, 155.08, 0.214, 2.065, 627.1, 1.5, 347, 3.44, 10, 1, 4264, 4.637, 0.62, 291.02, 36.91, 15.544]
      exoplanetprediction(k07622)

      The celestial object is not an exoplanet.
```

## 4.5 Exoplanet Habitability Prediction Using User Input

Similarly, the potential for habitability of existing exoplanets was also tested.

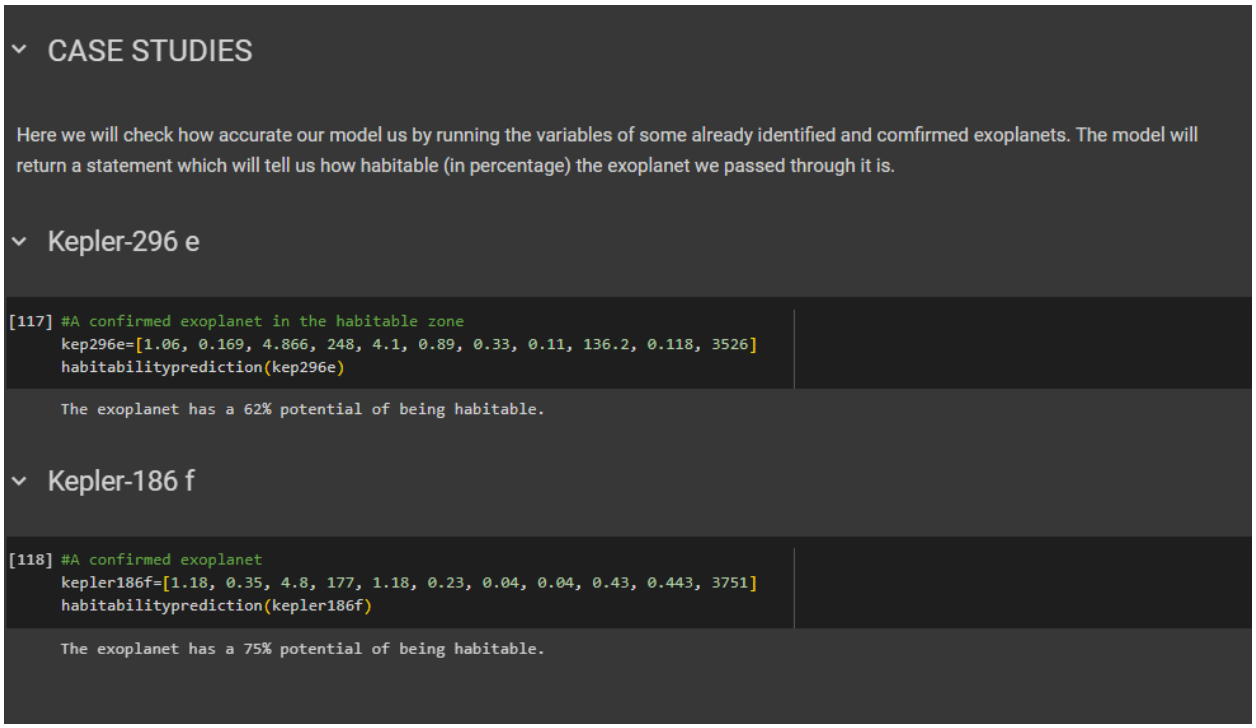


Link to the project: https://github.com/JahanviChamria/ExoplanetResearchProject

# 5. Discussion

In the report above, we discussed the various properties of exoplanets and exoplanet atmospheres, which make them habitable. We also discussed the basics of exoplanet sciences, detection methods, various models and history of achievements in exoplanet detection. The main criterion to determine if these planets are habitable is whether they lie in the habitable zone of their corresponding star. Taking into account these properties and the available data, a program using artificial intelligence was designed to help detect habitable exoplanets and conduct a comprehensive analysis.

## 6. Conclusion & Future Outlook

Till now, the search for habitable exoplanets has been guided solely on the basis of similarity to the Earth and the presence of Earth-like conditions, but we may also find exoplanets different from Earth possessing the ability to sustain life. This process will become much more efficient with the development of more tools and projects to view and analyze not only the stellar and planetary conditions but also the atmospheric conditions of exoplanets light years away. In our project, we have also used Earth as the standard for determining potential exoplanet habitability, but AI algorithms have made the process more accurate. Despite the absence of atmospheric data for a considerable number of exoplanets, there exists substantial promise for groundbreaking discoveries in this field.

## Acknowledgments

The research in this report was partially supported by Sarvesh Gharat, P.h.D student at the Centre for Machine Intelligence and Data Science, IIT Bombay. We thank our advisor for guidance throughout the research.

## Author contributions

Jahanvi Chamria*, Harshika Kerkar*, Riddhim Garg* and Sarvesh Gharat.
*These authors contributed equally to this work.

# References

[1] G. Bruno and P. Sanasi, [Online]. Available: http://www.ousia.it/content/Sezioni/Testi/BrunoDeInfinitoUniverso.pdf.

[2] "1979JHA....10...23H Page 23," adsabs.harvard.edu. https://adsabs.harvard.edu/full/1979JHA....10...23H.

[3] B. Campbell, G. A. H. Walker, and S. Yang, "A search for substellar companions to solar-type stars," The Astrophysical Journal, vol. 331, p. 902, Aug. 1988, doi: https://doi.org/10.1086/166608.

[4] M. Mayor and D. Queloz, "A Jupiter-mass companion to a solar-type star," Nature, vol. 378, no. 6555, pp. 355–359, Nov. 1995, doi: https://doi.org/10.1038/378355a0.

[5] C. Melis and P. Dufour, "DOES A DIFFERENTIATED, CARBONATE-RICH, ROCKY OBJECT POLLUTE THE WHITE DWARF SDSS J104341.53+085558.2?," The Astrophysical Journal, vol. 834, no. 1, p. 1, Dec. 2016, doi: https://doi.org/10.3847/1538-4357/834/1/1.

[6] N. Madhusudhan, "Exoplanetary Atmospheres: Key Insights, Challenges, and Prospects," Annual Review of Astronomy and Astrophysics, vol. 57, no. 1, pp. 617–663, Aug. 2019, doi: https://doi.org/10.1146/annurev-astro-081817-051846.

[7] S. Seager and W. Bains, "The search for signs of life on exoplanets at the interface of chemistry and planetary science," Science Advances, vol. 1, no. 2, p. e1500047, Mar. 2015, doi: https://doi.org/10.1126/sciadv.1500047.

[8] J. Horner et al., "Solar System Physics for Exoplanet Research," Publications of the Astronomical Society of the Pacific, vol. 132, no. 1016, p. 102001, Sep. 2020, doi: https://doi.org/10.1088/1538-3873/ab8eb9.

[9] C. Mordasini, "Planetary population synthesis," arXiv.org, 2018. https://arxiv.org/abs/1804.01532.

[10] "Project MUSE - Comparative Climatology of Terrestrial Planets," muse.jhu.edu. https://muse.jhu.edu/chapter/1207495.

[11] B. R. Oppenheimer and S. Hinkley, "High-Contrast Observations in Optical and Infrared Astronomy," Annual Review of Astronomy and Astrophysics, vol. 47, no. 1, pp. 253–289, Sep. 2009, doi: https://doi.org/10.1146/annurev-astro-082708-101717.

[12] "Life Sciences, Society and Policy," www.scimagojr.com. https://www.scimagojr.com/journalsearch.php?q=21100466413&tip=sid&clean=0

[13] M. Perryman, The Exoplanet Handbook, 2nd ed. Cambridge: Cambridge University Press, 2018. [Online]. Available: https://www.cambridge.org/core/books/exoplanet-handbook/750759E015FDCF469D141F0046198519.

[14] "Discoveries Dashboard | Discovery," *Exoplanet Exploration: Planets Beyond our Solar System*. https://exoplanets.nasa.gov/discovery/discoveries-dashboard/.

[15] "Historic Timeline | Explore," *Exoplanet Exploration: Planets Beyond our Solar System*. https://exoplanets.nasa.gov/alien-worlds/historic-timeline/#first-planetary-disk-observed.

[16] J. I. Lunine et al., “Worlds Beyond: A Strategy for the Detection and Characterization of Exoplanets,” arXiv (Cornell University), Aug. 2008, doi: https://doi.org/10.48550/arxiv.0808.2754.

[17] J. I. Lunine, B. Macintosh, and S. Peale, “The detection and characterization of exoplanets,” Physics Today, vol. 62, no. 5, pp. 46–51, May 2009, doi: https://doi.org/10.1063/1.3141941.

[18] J. T. Wright, G. W. Marcy, A. W. Howard, J. A. Johnson, T. D. Morton, and D. A. Fischer, “THE FREQUENCY OF HOT JUPITERS ORBITING NEARBY SOLAR-TYPE STARS,” The Astrophysical Journal, vol. 753, no. 2, p. 160, Jun. 2012, doi: https://doi.org/10.1088/0004-637x/753/2/160.

[19] D. M. Kipping, G. Á. Bakos, L. Buchhave, D. Nesvorný, and A. Schmitt, “THE HUNT FOR EXOMOONS WITHKEPLER(HEK). I. DESCRIPTION OF A NEW OBSERVATIONAL PROJECT,” The Astrophysical Journal, vol. 750, no. 2, p. 115, Apr. 2012, doi: https://doi.org/10.1088/0004-637x/750/2/115.

[20] N. Madhusudhan, H. Knutson, J. J. Fortney, and T. Barman, Exoplanetary Atmospheres. eprint: arXiv:1402.1169, 2014. [Online]. Available: https://ui.adsabs.harvard.edu/abs/2014prpl.conf..739M/abstract.

[21] D. P. Bennett and S. H. Rhie, “Detecting Earth-Mass Planets with Gravitational Microlensing,” The Astrophysical Journal, vol. 472, no. 2, pp. 660–664, Dec. 1996, doi: https://doi.org/10.1086/178096.

[22] “Spectroscopy Infographic,” Exoplanet Exploration: Planets Beyond our Solar System. https://exoplanets.nasa.gov/resources/2270/spectroscopy-infographic/

[23] “Exoplanet atmospheres - Department of Physics and Astronomy - Uppsala University, Sweden,” Physics.uu.se, 2019. https://www.physics.uu.se/research/astronomy-and-space-physics/research/planets/exoplanet-atmospheres/.

[24] L. D. Deming and S. Seager, “Illusion and reality in the atmospheres of exoplanets,” Journal of Geophysical Research: Planets, vol. 122, no. 1, pp. 53–75, Jan. 2017, doi: https://doi.org/10.1002/2016je005155.

[25] M. Richmond, “Spectroscopy of exoplanets,” spiff.rit.edu. http://spiff.rit.edu/classes/resceu/lectures/spectra/spectra.html.

[26] L. Kreidberg, “Exoplanet Atmosphere Measurements from Transmission Spectroscopy and other Planet-Star Combined Light Observations,” arXiv:1709.05941 [astro-ph], pp. 2083–2105, 2018, doi: https://doi.org/10.1007/978-3-319-55333-7_100.

[27] B. Charnay and P. Drossart, “Characterization and modelling of exoplanetary atmospheres,” Comptes Rendus Physique, vol. 24, no. S2, pp. 1–11, Apr. 2023, doi: https://doi.org/10.5802/crphys.143.

[28] J. Sarkar, K. Bhatia, S. Saha, M. Safonova, and S. Sarkar, “Postulating exoplanetary habitability via a novel anomaly detection method,” Monthly Notices of the Royal Astronomical Society, vol. 510, no. 4, pp. 6022–6032, Dec. 2021, doi: https://doi.org/10.1093/mnras/stab3556.

[29] P. Simonetti, G. Vladilo, L. Silva, and A. Sozzetti, “Statistical Properties of Habitable Zones in Stellar Binary Systems,” The Astrophysical Journal, vol. 903, no. 2, p. 141, Nov. 2020, doi: https://doi.org/10.3847/1538-4357/abc074.

[30] J. F. Kasting, R. Kopparapu, R. M. Ramirez, and C. E. Harman, “Remote life-detection criteria, habitable zone boundaries, and the frequency of Earth-like planets around M and late K stars,” Proceedings of the National Academy of Sciences, vol. 111, no. 35, pp. 12641–12646, Nov. 2013, doi: https://doi.org/10.1073/pnas.1309107110.

[31] D. J. Armstrong et al., “The Host Stars of Keplers Habitable Exoplanets: Superflares, Rotation and Activity,” Monthly Notices of the Royal Astronomical Society, vol. 455, no. 3, pp. 3110–3125, Jan. 2016, doi: https://doi.org/10.1093/mnras/stv2419.

[32] “The Goldilocks Zone ebook by Laura La Bella,” Rakuten Kobo. https://www.kobo.com/us/en/ebook/the-goldilocks-zone-2.

[33] T. Jansen, C. Scharf, M. Way, and A. Del Genio, “Climates of Warm Earth-like Planets. II. Rotational ‘Goldilocks’ Zones for Fractional Habitability and Silicate Weathering,” The Astrophysical Journal, vol. 875, no. 2, p. 79, Apr. 2019, doi: https://doi.org/10.3847/1538-4357/ab113d.

[34] C. Kilic, C. C. Raible, and T. F. Stocker, “Multiple Climate States of Habitable Exoplanets: The Role of Obliquity and Irradiance,” The Astrophysical Journal, vol. 844, no. 2, p. 147, Aug. 2017, doi: https://doi.org/10.3847/1538-4357/aa7a03.

[35] “Determining the Habitability of Exoplanets Surface Gravitational Acceleration.” Available: https://ulab.berkeley.edu/static/doc/posters/s181.pdf.

[36] “Exploring the Impact of Planetary Mass and Gravity on Habitability,” Space Mesmerise, May 17, 2023. https://spacemesmerise.com/en-in/blogs/astrobiology/exploring-the-impact-of-planetary-mass-and-gravity-on-habitability

[37] N. Madhusudhan, M. Agúndez, J. I. Moses, and Y. Hu, “Exoplanetary Atmospheres—Chemistry, Formation Conditions, and Habitability,” Space Science Reviews, May 12, 2016. [Online]. Available: https://doi.org/10.1007/s11214-016-0254-3.

[38] S. Matousek, “The Juno New Frontiers mission,” *Acta Astronautica*, Nov. 01, 2007. [Online]. Available: https://doi.org/10.1016/j.actaastro.2006.12.013.

[39] W. Norde, “Colloids and Interfaces in Life Sciences,” *CRC Press eBooks*, Jun. 20, 2003. [Online]. Available: https://doi.org/10.1201/9780203912157.

[40] J. E. Frederick and D. Lubin, “The budget of biologically active ultraviolet radiation in the Earth-atmosphere system,” *Journal of Geophysical Research*, vol. 93, no. D4, p. 3825, 1988, doi: 10.1029/jd093id04p03825. [Online]. Available: http://dx.doi.org/10.1029/jd093id04p03825.

[41] S. B. Curtis and J. R. Letaw, “Galactic cosmic rays and cell-hit frequencies outside the magnetosphere,” *Advances in Space Research*, vol. 9, no. 10, pp. 293–298, Jan. 1989, doi: 10.1016/0273-1177(89)90452-3. [Online]. Available: http://dx.doi.org/10.1016/0273-1177(89)90452-3.

[42] J. F. Kasting, “Earth’s Early Atmosphere,” *Science*, vol. 259, no. 5097, pp. 920–926, Feb. 1993, doi: 10.1126/science.11536547. [Online]. Available: http://dx.doi.org/10.1126/science.11536547.

[43] E. T. Sundquist, “The Global Carbon Dioxide Budget,” *Science*, vol. 259, no. 5097, pp. 934–941, Feb. 1993, doi: 10.1126/science.259.5097.934. [Online]. Available: http://dx.doi.org/10.1126/science.259.5097.934.

[44] D. Schulze-Makuch *et al.*, “A Two-Tiered Approach to Assessing the Habitability of Exoplanets,” *Astrobiology*, vol. 11, no. 10, pp. 1041–1052, Dec. 2011, doi: 10.1089/ast.2010.0592. [Online]. Available: http://dx.doi.org/10.1089/ast.2010.0592.

[45] J. F. Kasting and J. L. Siefert, “Life and the Evolution of Earth’s Atmosphere,” *Science*, vol. 296, no. 5570, pp. 1066–1068, May 2002, doi: 10.1126/science.1071184. [Online]. Available: http://dx.doi.org/10.1126/science.1071184.

[46] H. Lammer *et al.*, “Geophysical and Atmospheric Evolution of Habitable Planets,” *Astrobiology*, vol. 10, no. 1, pp. 45–68, Jan. 2010, doi: 10.1089/ast.2009.0368. [Online]. Available: http://dx.doi.org/10.1089/ast.2009.0368.

[47] C. H. Lineweaver, “W. T. Sullivan III & J. A. Baross (eds) 2007. Planets and Life. The Emerging Science of Astrobiology. xxi + 604 pp. Cambridge, New York, Melbourne: Cambridge University Press. Price £80.00, US $150.00 (hard covers), £40.00, US $75.00 (paperback). ISBN 9780 521 82421 7; 9780 521 53102 3 (pb).,” *Geological Magazine*, vol. 145, no. 4, pp. 607–607, Jun. 2008, doi: 10.1017/s0016756808004792. [Online]. Available: http://dx.doi.org/10.1017/s0016756808004792.

[48] J. F. Rowe *et al.*, “The Very Low Albedo of an Extrasolar Planet:MOSTSpace-based Photometry of HD 209458,” *The Astrophysical Journal*, vol. 689, no. 2, pp. 1345–1353, Dec. 2008, doi: 10.1086/591835. [Online]. Available: http://dx.doi.org/10.1086/591835.

[49] N. B. Cowan and E. Agol, “THE STATISTICS OF ALBEDO AND HEAT RECIRCULATION ON HOT EXOPLANETS,” *The Astrophysical Journal*, vol. 729, no. 1, p. 54, Feb. 2011, doi: 10.1088/0004-637x/729/1/54. [Online]. Available: http://dx.doi.org/10.1088/0004-637x/729/1/54.

[50] L. N. Irwin and D. Schulze-Makuch, “Life’s Fundamentals,” Nov. 19, 2010. [Online]. Available: https://doi.org/10.1007/978-1-4419-1647-1_3.

[51] A. Ekenbäck *et al.*, “ENERGETIC NEUTRAL ATOMS AROUND HD 209458b: ESTIMATIONS OF MAGNETOSPHERIC PROPERTIES,” *The Astrophysical Journal*, vol. 709, no. 2, pp. 670–679, Jan. 2010, doi: 10.1088/0004-637x/709/2/670. [Online]. Available: http://dx.doi.org/10.1088/0004-637x/709/2/670.

[52] A. A. Vidotto, M. Jardine, and Ch. Helling, “EARLY UV INGRESS IN WASP-12b: MEASURING PLANETARY MAGNETIC FIELDS,” *The Astrophysical Journal*, vol. 722, no. 2, pp. L168–L172, Sep. 2010, doi: 10.1088/2041-8205/722/2/l168. [Online]. Available: http://dx.doi.org/10.1088/2041-8205/722/2/l168.

[53] L. N. Irwin and D. Schulze-Makuch, “Assessing the Plausibility of Life on Other Worlds,” *Astrobiology*, vol. 1, no. 2, pp. 143–160, Jun. 2001, doi: 10.1089/153110701753198918. [Online]. Available: http://dx.doi.org/10.1089/153110701753198918.

[54] “Life in the Universe: Expectations and Constraints, by D. Schulze-Makuch and L. N. Irwin.,” *Astrobiology*, vol. 4, no. 3, pp. 406–407, Jul. 2004, doi: 10.1089/1531107041939448. [Online]. Available: http://dx.doi.org/10.1089/1531107041939448.

[55] D. Schulze-Makuch and D. H. Grinspoon, “Biologically Enhanced Energy and Carbon Cycling on Titan?,” *Astrobiology*, vol. 5, no. 4, pp. 560–567, Aug. 2005, doi: 10.1089/ast.2005.5.560. [Online]. Available: http://dx.doi.org/10.1089/ast.2005.5.560.

[56] R. D. Wolstencroft and J. A. Raven, “Photosynthesis: Likelihood of Occurrence and Possibility of Detection on Earth-like Planets,” *Icarus*, vol. 157, no. 2, pp. 535–548, Jun. 2002, doi: 10.1006/icar.2002.6854. [Online]. Available: http://dx.doi.org/10.1006/icar.2002.6854.

[57] A. W. J. Muller, “Were the first organisms heat engines? A new model for biogenesis and the early evolution of biological energy conversion,” *Progress in Biophysics and Molecular Biology*, vol. 63, no. 2, pp. 193–231, 1995, doi: 10.1016/0079-6107(95)00004-7. [Online]. Available: http://dx.doi.org/10.1016/0079-6107(95)00004-7.

[58] V. S. Meadows and D. Crisp, “Ground-based near-infrared observations of the Venus nightside: The thermal structure and water abundance near the surface,” *Journal of Geophysical Research: Planets*, vol. 101, no. E2, pp. 4595–4622, Feb. 1996, doi: 10.1029/95je03567. [Online]. Available: http://dx.doi.org/10.1029/95je03567.

[59] N. Mueller *et al.*, “Venus surface thermal emission at 1μm in VIRTIS imaging observations: Evidence for variation of crust and mantle differentiation conditions,” *Journal of Geophysical Research*, vol. 113, Dec. 2008, doi: 10.1029/2008je003118. [Online]. Available: http://dx.doi.org/10.1029/2008je003118.

[60] T. Schindler, “Synthetic Spectra of Simulated Terrestrial Atmospheres Containing Possible Biomarker Gases,” *Icarus*, vol. 145, no. 1, pp. 262–271, May 2000, doi: 10.1006/icar.2000.6340. [Online]. Available: http://dx.doi.org/10.1006/icar.2000.6340.

[61] M. M. Joshi, R. M. Haberle, and R. T. Reynolds, “Simulations of the Atmospheres of Synchronously Rotating Terrestrial Planets Orbiting M Dwarfs: Conditions for Atmospheric Collapse and the Implications for Habitability,” *Icarus*, vol. 129, no. 2, pp. 450–465, Oct. 1997, doi: 10.1006/icar.1997.5793. [Online]. Available: http://dx.doi.org/10.1006/icar.1997.5793.

[62] F. Westall *et al.*, “Polymeric substances and biofilms as biomarkers in terrestrial materials: Implications for extraterrestrial samples,” *Journal of Geophysical Research: Planets*, vol. 105, no. E10, pp. 24511–24527, Oct. 2000, doi: 10.1029/2000je001250. [Online]. Available: http://dx.doi.org/10.1029/2000je001250.

[63] N. R. Pace, “The universal nature of biochemistry,” *Proceedings of the National Academy of Sciences*, vol. 98, no. 3, pp. 805–808, Jan. 2001, doi: 10.1073/pnas.98.3.805. [Online]. Available: http://dx.doi.org/10.1073/pnas.98.3.805.

[64] W. Bains, “Many Chemistries Could Be Used to Build Living Systems,” *Astrobiology*, vol. 4, no. 2, pp. 137–167, Jun. 2004, doi: 10.1089/153110704323175124. [Online]. Available: http://dx.doi.org/10.1089/153110704323175124.

[65] S. A. Benner, A. Ricardo, and M. A. Carrigan, “Is there a common chemical model for life in the universe?,” *Current Opinion in Chemical Biology*, vol. 8, no. 6, pp. 672–689, Dec. 2004, doi: 10.1016/j.cbpa.2004.10.003. [Online]. Available: http://dx.doi.org/10.1016/j.cbpa.2004.10.003.

[66] J. D. Anderson, G. Schubert, R. A. Jacobson, E. L. Lau, W. B. Moore, and W. L. Sjogren, “Europa’s Differentiated Internal Structure: Inferences from Four Galileo Encounters,” *Science*, vol. 281, no. 5385, pp. 2019–2022, Sep. 1998, doi: 10.1126/science.281.5385.2019. [Online]. Available: http://dx.doi.org/10.1126/science.281.5385.2019.

[67] C. C. Porco *et al.*, “Cassini Observes the Active South Pole of Enceladus,” *Science*, vol. 311, no. 5766, pp. 1393–1401, Mar. 2006, doi: 10.1126/science.1123013. [Online]. Available: http://dx.doi.org/10.1126/science.1123013.

[68] A. Burrows and C. M. Sharp, “Chemical Equilibrium Abundances in Brown Dwarf and Extrasolar Giant Planet Atmospheres,” The Astrophysical Journal, vol. 512, no. 2, pp. 843–863, Feb. 1999, doi: 10.1086/306811. [Online]. Available: http://dx.doi.org/10.1086/306811.

[69] C. Visscher, K. Lodders, and B. Fegley, Jr., “Atmospheric Chemistry in Giant Planets, Brown Dwarfs, and Low-Mass Dwarf Stars. II. Sulfur and Phosphorus,” The Astrophysical Journal, vol. 648, no. 2, pp. 1181–1195, Sep. 2006, doi: 10.1086/506245. [Online]. Available: http://dx.doi.org/10.1086/506245.

[70] J. I. Moses et al., “COMPOSITIONAL DIVERSITY IN THE ATMOSPHERES OF HOT NEPTUNES, WITH APPLICATION TO GJ 436b,” The Astrophysical Journal, vol. 777, no. 1, p. 34, Oct. 2013, doi: 10.1088/0004-637x/777/1/34. [Online]. Available: http://dx.doi.org/10.1088/0004-637x/777/1/34.

[71] J. J. Fortney, M. S. Marley, and J. W. Barnes, “Planetary Radii across Five Orders of Magnitude in Mass and Stellar Insolation: Application to Transits,” The Astrophysical Journal, vol. 659, no. 2, pp. 1661–1672, Apr. 2007, doi: 10.1086/512120. [Online]. Available: http://dx.doi.org/10.1086/512120.

[72] A. Lecavelier des Etangs, F. Pont, A. Vidal-Madjar, and D. Sing, “Rayleigh scattering in the transit spectrum of HD 189733b,” Astronomy & Astrophysics, vol. 481, no. 2, pp. L83–L86, Feb. 2008, doi: 10.1051/0004-6361:200809388. [Online]. Available: http://dx.doi.org/10.1051/0004-6361:200809388.

[73] J. Patience, R. R. King, R. J. De Rosa, and C. Marois, “The highest resolution near infrared spectrum of the imaged planetary mass companion 2M1207 b,” Astronomy and Astrophysics, vol. 517, p. A76, Jul. 2010, doi: 10.1051/0004-6361/201014173. [Online]. Available: http://dx.doi.org/10.1051/0004-6361/201014173.

[74] J. Gagné, D. Lafrenière, R. Doyon, L. Malo, and É. Artigau, “BANYAN. II. VERY LOW MASS AND SUBSTELLAR CANDIDATE MEMBERS TO NEARBY, YOUNG KINEMATIC GROUPS WITH PREVIOUSLY KNOWN SIGNS OF YOUTH,” The Astrophysical Journal, vol. 783, no. 2, p. 121, Feb. 2014, doi: 10.1088/0004-637x/783/2/121. [Online]. Available: http://dx.doi.org/10.1088/0004-637x/783/2/121.

[75] M. Bonnefoy et al., “Physical and orbital properties ofβPictoris b,” Astronomy & Astrophysics, vol. 567, p. L9, Jul. 2014, doi: 10.1051/0004-6361/201424041. [Online]. Available: http://dx.doi.org/10.1051/0004-6361/201424041.

[76] T. S. Barman, Q. M. Konopacky, B. Macintosh, and C. Marois, “SIMULTANEOUS DETECTION OF WATER, METHANE, AND CARBON MONOXIDE IN THE ATMOSPHERE OF EXOPLANET HR 8799 b,” The Astrophysical Journal, vol. 804, no. 1, p. 61, May 2015, doi: 10.1088/0004-637x/804/1/61. [Online]. Available: http://dx.doi.org/10.1088/0004-637x/804/1/61.

[77] A. C. Lockwood et al., “NEAR-IR DIRECT DETECTION OF WATER VAPOR IN TAU BOÖTIS b,” The Astrophysical Journal, vol. 783, no. 2, p. L29, Feb. 2014, doi: 10.1088/2041-8205/783/2/l29. [Online]. Available: http://dx.doi.org/10.1088/2041-8205/783/2/l29.

[78] M. Brogi, R. J. de Kok, J. L. Birkby, H. Schwarz, and I. A. G. Snellen, “Carbon monoxide and water vapor in the atmosphere of the non-transiting exoplanet HD 179949 b,” Astronomy & Astrophysics, vol. 565, p. A124, May 2014, doi: 10.1051/0004-6361/201423537. [Online]. Available: http://dx.doi.org/10.1051/0004-6361/201423537.

[79] J. L. Birkby et al., “Detection of water absorption in the day side atmosphere of HD 189733 b using ground-based high-resolution spectroscopy at 3.2 μm★,” Monthly Notices of the Royal Astronomical Society: Letters, vol. 436, no. 1, pp. L35–L39, Aug. 2013, doi: 10.1093/mnrasl/slt107. [Online]. Available: http://dx.doi.org/10.1093/mnrasl/slt107.

[80] S. K. Leggett, C. V. Morley, M. S. Marley, D. Saumon, J. J. Fortney, and C. Visscher, “A COMPARISON OF NEAR-INFRARED PHOTOMETRY AND SPECTRA FOR Y DWARFS WITH A NEW GENERATION OF COOL CLOUDY MODELS,” The Astrophysical Journal, vol. 763, no. 2, p. 130, Jan. 2013, doi: 10.1088/0004-637x/763/2/130. [Online]. Available: http://dx.doi.org/10.1088/0004-637x/763/2/130.

[81] M. R. Line, J. J. Fortney, M. S. Marley, and S. Sorahana, “A DATA-DRIVEN APPROACH FOR RETRIEVING TEMPERATURES AND ABUNDANCES IN BROWN DWARF ATMOSPHERES,” The Astrophysical Journal, vol. 793, no. 1, p. 33, Sep. 2014, doi: 10.1088/0004-637x/793/1/33. [Online]. Available: http://dx.doi.org/10.1088/0004-637x/793/1/33.

[82] M. R. Line, J. Teske, B. Burningham, J. J. Fortney, and M. S. Marley, “UNIFORM ATMOSPHERIC RETRIEVAL ANALYSIS OF ULTRACOOL DWARFS. I. CHARACTERIZING BENCHMARKS, Gl 570D AND HD 3651B,” The Astrophysical Journal, vol. 807, no. 2, p. 183, Jul. 2015, doi: 10.1088/0004-637x/807/2/183. [Online]. Available: http://dx.doi.org/10.1088/0004-637x/807/2/183.

[83] I. N. Reid and S. L. Hawley, “New Light on Dark Stars,” 2005, doi: 10.1007/3-540-27610-6. [Online]. Available: http://dx.doi.org/10.1007/3-540-27610-6.

[84] J.-M. Désert et al., “TiO and VO broad band absorption features in the optical spectrum of the atmosphere of the hot-Jupiter HD 209458b,” Astronomy & Astrophysics, vol. 492, no. 2, pp. 585–592, Oct. 2008, doi: 10.1051/0004-6361:200810355. [Online]. Available: http://dx.doi.org/10.1051/0004-6361:200810355.

[85] H. J. Hoeijmakers, R. J. de Kok, I. A. G. Snellen, M. Brogi, J. L. Birkby, and H. Schwarz, “A search for TiO in the optical high-resolution transmission spectrum of HD 209458b: Hindrance due to inaccuracies in the line database,” Astronomy & Astrophysics, vol. 575, p. A20, Feb. 2015, doi: 10.1051/0004-6361/201424794. [Online]. Available: http://dx.doi.org/10.1051/0004-6361/201424794.

[86] H. A. Knutson et al., “ASPITZERTRANSMISSION SPECTRUM FOR THE EXOPLANET GJ 436b, EVIDENCE FOR STELLAR VARIABILITY, AND CONSTRAINTS ON DAYSIDE FLUX VARIATIONS,” The Astrophysical Journal, vol. 735, no. 1, p. 27, Jun. 2011, doi: 10.1088/0004-637x/735/1/27. [Online]. Available: http://dx.doi.org/10.1088/0004-637x/735/1/27.

[87] F. Pont, D. K. Sing, N. P. Gibson, S. Aigrain, G. Henry, and N. Husnoo, “The prevalence of dust on the exoplanet HD 189733b from Hubble and Spitzer observations,” Monthly Notices of the Royal Astronomical Society, vol. 432, no. 4, pp. 2917–2944, May 2013, doi: 10.1093/mnras/stt651. [Online]. Available: http://dx.doi.org/10.1093/mnras/stt651.

[88] J. K. Barstow, S. Aigrain, P. G. J. Irwin, S. Kendrew, and L. N. Fletcher, “Transit spectroscopy with James Webb Space Telescope: systematics, starspots and stitching,” Monthly Notices of the Royal Astronomical Society, vol. 448, no. 3, pp. 2546–2561, Mar. 2015, doi: 10.1093/mnras/stv186. [Online]. Available: http://dx.doi.org/10.1093/mnras/stv186.

[89] C. J. Hansen, J. C. Schwartz, and N. B. Cowan, “Features in the broad-band eclipse spectra of exoplanets: signal or noise?,” Monthly Notices of the Royal Astronomical Society, vol. 444, no. 4, pp. 3632–3640, Sep. 2014, doi: 10.1093/mnras/stu1699. [Online]. Available: http://dx.doi.org/10.1093/mnras/stu1699.

[90] L. Kaltenegger and W. A. Traub, “TRANSITS OF EARTH-LIKE PLANETS,” The Astrophysical Journal, vol. 698, no. 1, pp. 519–527, May 2009, doi: 10.1088/0004-637x/698/1/519. [Online]. Available: http://dx.doi.org/10.1088/0004-637x/698/1/519.

[91] D. Deming et al., “Discovery and Characterization of Transiting Super Earths Using an All-Sky Transit Survey and Follow-up by theJames Webb Space Telescope,” Publications of the Astronomical Society of the Pacific, vol. 121, no. 883, pp. 952–967, Sep. 2009, doi: 10.1086/605913. [Online]. Available: http://dx.doi.org/10.1086/605913.

[92] M. Asplund, N. Grevesse, A. J. Sauval, and P. Scott, “The Chemical Composition of the Sun,” Annual Review of Astronomy and Astrophysics, vol. 47, no. 1, pp. 481–522, Sep. 2009, doi: 10.1146/annurev.astro.46.060407.145222. [Online]. Available: http://dx.doi.org/10.1146/annurev.astro.46.060407.145222.

[93] N. Madhusudhan, H. Knutson, J. J. Fortney, and T. Barman, “Exoplanetary Atmospheres,” University of Arizona Press eBooks, Jan. 01, 2014. [Online]. Available: https://doi.org/10.2458/azu_uapress_9780816531240-ch032.

[94] K. Heng and A. P. Showman, “Atmospheric Dynamics of Hot Exoplanets,” Annual Review of Earth and Planetary Sciences, vol. 43, no. 1, pp. 509–540, May 2015, doi: 10.1146/annurev-earth-060614-105146. [Online]. Available: http://dx.doi.org/10.1146/annurev-earth-060614-105146.

[95] Q. M. Konopacky, T. S. Barman, B. A. Macintosh, and C. Marois, “Detection of Carbon Monoxide and Water Absorption Lines in an Exoplanet Atmosphere,” Science, vol. 339, no. 6126, pp. 1398–1401, Mar. 2013, doi: 10.1126/science.1232003. [Online]. Available: http://dx.doi.org/10.1126/science.1232003.

[96] N. B. Cowan et al., “THERMAL PHASE VARIATIONS OF WASP-12b: DEFYING PREDICTIONS,” The Astrophysical Journal, vol. 747, no. 1, p. 82, Feb. 2012, doi: 10.1088/0004-637x/747/1/82. [Online]. Available: http://dx.doi.org/10.1088/0004-637x/747/1/8.

[97] I. J. M. Crossfield, T. Barman, B. M. S. Hansen, I. Tanaka, and T. Kodama, “RE-EVALUATING WASP-12b: STRONG EMISSION AT 2.315 μm, DEEPER OCCULTATIONS, AND AN ISOTHERMAL ATMOSPHERE,” The Astrophysical Journal, vol. 760, no. 2, p. 140, Nov. 2012, doi: 10.1088/0004-637x/760/2/140. [Online]. Available: http://dx.doi.org/10.1088/0004-637x/760/2/140.

[98] M. Swain et al., “Probing the extreme planetary atmosphere of WASP-12b,” Icarus, vol. 225, no. 1, pp. 432–445, Jul. 2013, doi: 10.1016/j.icarus.2013.04.003. [Online]. Available: http://dx.doi.org/10.1016/j.icarus.2013.04.003.

[99] E. B. Bechter et al., “WASP-12b AND HAT-P-8b ARE MEMBERS OF TRIPLE STAR SYSTEMS,” The Astrophysical Journal, vol. 788, no. 1, p. 2, May 2014, doi: 10.1088/0004-637x/788/1/2. [Online]. Available: http://dx.doi.org/10.1088/0004-637x/788/1/2.

[100] M. R. Line, H. Knutson, A. S. Wolf, and Y. L. Yung, “A SYSTEMATIC RETRIEVAL ANALYSIS OF SECONDARY ECLIPSE SPECTRA. II. A UNIFORM ANALYSIS OF NINE PLANETS AND THEIR C TO O RATIOS,” The Astrophysical Journal, vol. 783, no. 2, p. 70, Feb. 2014, doi: 10.1088/0004-637x/783/2/70. [Online]. Available: http://dx.doi.org/10.1088/0004-637x/783/2/70.

[101] K. B. Stevenson, J. L. Bean, N. Madhusudhan, and J. Harrington, “DECIPHERING THE ATMOSPHERIC COMPOSITION OF WASP-12b: A COMPREHENSIVE ANALYSIS OF ITS DAYSIDE EMISSION,” The Astrophysical Journal, vol. 791, no. 1, p. 36, Jul. 2014, doi: 10.1088/0004-637x/791/1/36. [Online]. Available: http://dx.doi.org/10.1088/0004-637x/791/1/36.

[102] S. Chapman, “XXXV.On ozone and atomic oxygen in the upper atmosphere,” The London, Edinburgh, and Dublin Philosophical Magazine and Journal of Science, vol. 10, no. 64, pp. 369–383, Sep. 1930, doi: 10.1080/14786443009461588. [Online]. Available: http://dx.doi.org/10.1080/14786443009461588.

[103] J. I. Moses et al., “DISEQUILIBRIUM CARBON, OXYGEN, AND NITROGEN CHEMISTRY IN THE ATMOSPHERES OF HD 189733b AND HD 209458b,” The Astrophysical Journal, vol. 737, no. 1, p. 15, Jul. 2011, doi: 10.1088/0004-637x/737/1/15. [Online]. Available: http://dx.doi.org/10.1088/0004-637x/737/1/15.

[104] Y. Miguel and L. Kaltenegger, “EXPLORING ATMOSPHERES OF HOT MINI-NEPTUNES AND EXTRASOLAR GIANT PLANETS ORBITING DIFFERENT STARS WITH APPLICATION TO HD 97658b, WASP-12b, CoRoT-2b, XO-1b, AND HD 189733b,” The Astrophysical Journal, Dec. 20, 2013. [Online]. Available: https://doi.org/10.1088/0004-637x/780/2/166.

[105] K. Haynes, A. M. Mandell, N. Madhusudhan, D. Deming, and H. Knutson, “SPECTROSCOPIC EVIDENCE FOR A TEMPERATURE INVERSION IN THE DAYSIDE ATMOSPHERE OF HOT JUPITER WASP-33b,” The Astrophysical Journal, vol. 806, no. 2, p. 146, Jun. 2015, doi: 10.1088/0004-637x/806/2/146. [Online]. Available: http://dx.doi.org/10.1088/0004-637x/806/2/146.

[106] I. J. M. Crossfield, “Observations of Exoplanet Atmospheres,” Publications of the Astronomical Society of the Pacific, vol. 127, no. 956, pp. 941–960, Oct. 2015, doi: 10.1086/683115. [Online]. Available: http://dx.doi.org/10.1086/683115.

[107] T. S. Barman, B. Macintosh, Q. M. Konopacky, and C. Marois, “CLOUDS AND CHEMISTRY IN THE ATMOSPHERE OF EXTRASOLAR PLANET HR8799b,” The Astrophysical Journal, vol. 733, no. 1, p. 65, May 2011, doi: 10.1088/0004-637x/733/1/65. [Online]. Available: http://dx.doi.org/10.1088/0004-637x/733/1/65.

[108] T. S. Barman, Q. M. Konopacky, B. Macintosh, and C. Marois, “SIMULTANEOUS DETECTION OF WATER, METHANE, AND CARBON MONOXIDE IN THE ATMOSPHERE OF EXOPLANET HR 8799 b,” The Astrophysical Journal, vol. 804, no. 1, p. 61, May 2015, doi: 10.1088/0004-637x/804/1/61. [Online]. Available: http://dx.doi.org/10.1088/0004-637x/804/1/61.

[109] J.-M. Lee, K. Heng, and P. G. J. Irwin, “ATMOSPHERIC RETRIEVAL ANALYSIS OF THE DIRECTLY IMAGED EXOPLANET HR 8799b,” The Astrophysical Journal, vol. 778, no. 2, p. 97, Nov. 2013, doi: 10.1088/0004-637x/778/2/97. [Online]. Available: http://dx.doi.org/10.1088/0004-637x/778/2/97.

[110] A. J. Skemer et al., “DIRECTLY IMAGED L-T TRANSITION EXOPLANETS IN THE MID-INFRARED,” The Astrophysical Journal, vol. 792, no. 1, p. 17, Aug. 2014, doi: 10.1088/0004-637x/792/1/17. [Online]. Available: http://dx.doi.org/10.1088/0004-637x/792/1/17.

[111] P. Lavvas, T. Koskinen, and R. V. Yelle, “ELECTRON DENSITIES AND ALKALI ATOMS IN EXOPLANET ATMOSPHERES,” The Astrophysical Journal, vol. 796, no. 1, p. 15, Oct. 2014, doi: 10.1088/0004-637x/796/1/15. [Online]. Available: http://dx.doi.org/10.1088/0004-637x/796/1/15.

[112] D. Charbonneau, T. M. Brown, R. W. Noyes, and R. L. Gilliland, “Detection of an Extrasolar Planet Atmosphere,” The Astrophysical Journal, vol. 568, no. 1, pp. 377–384, Mar. 2002, doi: 10.1086/338770. [Online]. Available: http://dx.doi.org/10.1086/338770.

[113] S. Redfield, M. Endl, W. D. Cochran, and L. Koesterke, “Sodium Absorption from the Exoplanetary Atmosphere of HD 189733b Detected in the Optical Transmission Spectrum,” The Astrophysical Journal, vol. 673, no. 1, pp. L87–L90, Jan. 2008, doi: 10.1086/527475. [Online]. Available: http://dx.doi.org/10.1086/527475.

[114] J. F. Kasting, J. B. Pollack, and D. Crisp, “Effects of high CO2 levels on surface temperature and atmospheric oxidation state of the early Earth,” Journal of Atmospheric Chemistry, vol. 1, no. 4, pp. 403–428, 1984, doi: 10.1007/bf00053803. [Online]. Available: http://dx.doi.org/10.1007/bf00053803.

[115] J. F. Kasting and T. P. Ackerman, “Climatic Consequences of Very High Carbon Dioxide Levels in the Earth’s Early Atmosphere,” Science, vol. 234, no. 4782, pp. 1383–1385, Dec. 1986, doi: 10.1126/science.11539665. [Online]. Available: http://dx.doi.org/10.1126/science.11539665.

[116] J. F. Kasting, “Theoretical constraints on oxygen and carbon dioxide concentrations in the Precambrian atmosphere,” Precambrian Research, vol. 34, no. 3–4, pp. 205–229, Jan. 1987, doi: 10.1016/0301-9268(87)90001-5. [Online]. Available: http://dx.doi.org/10.1016/0301-9268(87)90001-5.

[117] J. F. Kasting, “Runaway and moist greenhouse atmospheres and the evolution of Earth and Venus,” Icarus, vol. 74, no. 3, pp. 472–494, Jun. 1988, doi: 10.1016/0019-1035(88)90116-9. [Online]. Available: http://dx.doi.org/10.1016/0019-1035(88)90116-9.

[118] J. F. Kasting, D. P. Whitmire, and R. T. Reynolds, “Habitable Zones around Main Sequence Stars,” Icarus, vol. 101, no. 1, pp. 108–128, Jan. 1993, doi: 10.1006/icar.1993.1010. [Online]. Available: http://dx.doi.org/10.1006/icar.1993.1010.

[119] J. F. Kasting, H. Chen, and R. K. Kopparapu, “STRATOSPHERIC TEMPERATURES AND WATER LOSS FROM MOIST GREENHOUSE ATMOSPHERES OF EARTH-LIKE PLANETS,” The Astrophysical Journal, vol. 813, no. 1, p. L3, Oct. 2015, doi: 10.1088/2041-8205/813/1/l3. [Online]. Available: http://dx.doi.org/10.1088/2041-8205/813/1/l3.

[120] A. A. Pavlov, J. F. Kasting, L. L. Brown, K. A. Rages, and R. Freedman, “Greenhouse warming by CH4in the atmosphere of early Earth,” Journal of Geophysical Research: Planets, vol. 105, no. E5, pp. 11981–11990, May 2000, doi: 10.1029/1999je001134. [Online]. Available: http://dx.doi.org/10.1029/1999je001134.

[121] A. A. Pavlov, M. T. Hurtgen, J. F. Kasting, and M. A. Arthur, “Methane-rich Proterozoic atmosphere?,” Geology, vol. 31, no. 1, p. 87, 2003 [Online]. Available: http://dx.doi.org/10.1130/0091-7613(2003)031.

[122] J. F. Kasting and M. T. Howard, “Atmospheric composition and climate on the early Earth,” Philosophical Transactions of the Royal Society B: Biological Sciences, vol. 361, no. 1474, pp. 1733–1742, Sep. 2006, doi: 10.1098/rstb.2006.1902. [Online]. Available: http://dx.doi.org/10.1098/rstb.2006.1902.

[123] J. D. Haqq-Misra, S. D. Domagal-Goldman, P. J. Kasting, and J. F. Kasting, “A Revised, Hazy Methane Greenhouse for the Archean Earth,” Astrobiology, vol. 8, no. 6, pp. 1127–1137, Dec. 2008, doi: 10.1089/ast.2007.0197. [Online]. Available: http://dx.doi.org/10.1089/ast.2007.0197.

[124] R. K. Kopparapu et al., “HABITABLE ZONES AROUND MAIN-SEQUENCE STARS: NEW ESTIMATES,” The Astrophysical Journal, vol. 765, no. 2, p. 131, Feb. 2013, doi: 10.1088/0004-637x/765/2/131. [Online]. Available: http://dx.doi.org/10.1088/0004-637x/765/2/131.

[125] G. Arney et al., “The Pale Orange Dot: The Spectrum and Habitability of Hazy Archean Earth,” Astrobiology, vol. 16, no. 11, pp. 873–899, Nov. 2016, doi: 10.1089/ast.2015.1422. [Online]. Available: http://dx.doi.org/10.1089/ast.2015.1422.

[126] G. N. Arney et al., “Pale Orange Dots: The Impact of Organic Haze on the Habitability and Detectability of Earthlike Exoplanets,” The Astrophysical Journal, vol. 836, no. 1, p. 49, Feb. 2017, doi: 10.3847/1538-4357/836/1/49. [Online]. Available: http://dx.doi.org/10.3847/1538-4357/836/1/49.

[127] C. Goldblatt and K. J. Zahnle, “Clouds and the Faint Young Sun Paradox,” Climate of the Past, vol. 7, no. 1, pp. 203–220, Mar. 2011, doi: 10.5194/cp-7-203-2011. [Online]. Available: http://dx.doi.org/10.5194/cp-7-203-2011.

[128] T. Fauchez, G. Arney, R. Kumar Kopparapu, and S. Domagal Goldman, “Explicit cloud representation in the Atmos 1D climate model for Earth and rocky planet applications,” AIMS Geosciences, vol. 4, no. 4, pp. 180–191, 2018, doi: 10.3934/geosci.2018.4.180. [Online]. Available: http://dx.doi.org/10.3934/geosci.2018.4.180.

[129] E. Roeckner et al., “Model description,” 2003.[Online]. Available: https://pure.mpg.de/rest/items/item_995269_4/component/file_995268/content.

[130] E. Roeckner et al., “Sensitivity of Simulated Climate to Horizontal and Vertical Resolution in the ECHAM5 Atmosphere Model,” Journal of Climate, vol. 19, no. 16, pp. 3771–3791, Aug. 2006, doi: https://doi.org/10.1175/jcli3824.1.

[131] M. Giorgetta et al., “Berichte zur Erdsystemforschung The atmospheric general circulation model ECHAM6 Model description,” 2013. [Online]. Available: https://pure.mpg.de/rest/items/item_1810480/component/file_1810481/content.

[132] B. Ruiz Cobo and J. C. del Toro Iniesta, “Inversion of Stokes profiles,” The Astrophysical Journal, vol. 398, p. 375, Oct. 1992, doi: 10.1086/171862. [Online]. Available: http://dx.doi.org/10.1086/171862.

[133] H. Socas-Navarro, “A high-resolution three-dimensional model of the solar photosphere derived from Hinode observations,” Astronomy & Astrophysics, vol. 529, p. A37, Mar. 2011, doi: 10.1051/0004-6361/201015805. [Online]. Available: http://dx.doi.org/10.1051/0004-6361/201015805.

[134] M. Asplund, Å. Nordlund, R. Trampedach, and R. Stein, “3D hydrodynamical model atmospheres of metal-poor stars Evidence for a low primordial Li abundance,” 1999. [Online]. Available: https://arxiv.org/pdf/astro-ph/9905059.pdf.

[135] R. Collet, M. Asplund, and R. Trampedach, “The Chemical Compositions of the Extreme Halo Stars HE 0107-5240 and HE 1327-2326 Inferred from Three-dimensional Hydrodynamical Model Atmospheres,” The Astrophysical Journal, vol. 644, no. 2, pp. L121–L124, Jun. 2006, doi: 10.1086/505643. [Online]. Available: http://dx.doi.org/10.1086/505643.

[136] R. Collet, M. Asplund, and R. Trampedach, “Three-dimensional hydrodynamical simulations of surface convection in red giant stars,” Astronomy & Astrophysics, vol. 469, no. 2, pp. 687–706, Apr. 2007, doi: 10.1051/0004-6361:20066321. [Online]. Available: http://dx.doi.org/10.1051/0004-6361:20066321.

[137] M. Asplund, Å. Nordlund, R. Trampedach, and R. Stein, “3D hydrodynamical model atmospheres of metal-poor stars Evidence for a low primordial Li abundance,” 1999. Available: https://arxiv.org/pdf/astro-ph/9905059.pdf.

[138] E. Caffau, H.-G. Ludwig, M. Steffen, B. Freytag, and P. Bonifacio, “Solar Chemical Abundances Determined with a CO5BOLD 3D Model Atmosphere,” Solar Physics, vol. 268, no. 2, pp. 255–269, Mar. 2010, doi: 10.1007/s11207-010-9541-4. [Online]. Available: http://dx.doi.org/10.1007/s11207-010-9541-4.

[139] R. Collet, Å. Nordlund, M. Asplund, W. Hayek, and R. Trampedach, “Memorie della ÙÒ Ò Ò ÐÝ× × Ó Ø À ÐÓ ÒØ À ½¾¾ ¿ Û Ø Ì Ö 1 Ñ Ò× ÓÒ Ð ÅÓ Ð ËØ ÐÐ Ö ØÑÓ×Ô Ö ×,” Mem. S.A.It, vol. 79, p. 1, 2009, [Online]. Available: https://arxiv.org/pdf/0909.0690.

[140] J. I. González Hernández, P. Bonifacio, H.-G. Ludwig, E. Caffau, N. T. Behara, and B. Freytag, “Galactic evolution of oxygen,” Astronomy and Astrophysics, vol. 519, p. A46, Sep. 2010, doi: 10.1051/0004-6361/201014397. [Online]. Available: http://dx.doi.org/10.1051/0004-6361/201014397.

[141] A. Frebel, R. Collet, K. Eriksson, N. Christlieb, and W. Aoki, “HE 1327−2326, an Unevolved Star with [Fe/H]<−5.0. II. New 3D−1D Corrected Abundances from a Very Large Telescope UVES Spectrum,” The Astrophysical Journal, vol. 684, no. 1, pp. 588–602, Sep. 2008, doi: 10.1086/590327. [Online]. Available: http://dx.doi.org/10.1086/590327.

[142] C. Rosenthal, J. Christensen-Dalsgaard, Å. Nordlund, R. Stein, and R. Trampedach, “ASTRONOMY AND ASTROPHYSICS Convective contributions to the frequencies of solar oscillations,” 1999. [Online]. Available: https://arxiv.org/pdf/astro-ph/9803206.pdf.

[143] A. Nordlund and R. F. Stein, “Solar Oscillations and Convection. I. Formalism for Radial Oscillations,” The Astrophysical Journal, vol. 546, no. 1, pp. 576–584, Jan. 2001, doi: 10.1086/318217. [Online]. Available: http://dx.doi.org/10.1086/318217.

[144] R. F. Stein and A. Nordlund, “Solar Oscillations and Convection. II. Excitation of Radial Oscillations,” The Astrophysical Journal, vol. 546, no. 1, pp. 585–603, Jan. 2001, doi: 10.1086/318218. [Online]. Available: http://dx.doi.org/10.1086/318218.

[145] Z. Magic et al., “The Stagger-grid: A grid of 3D stellar atmosphere models,” Astronomy and Astrophysics, vol. 557, pp. A26–A26, Aug. 2013, doi: https://doi.org/10.1051/0004-6361/201321274.

[146] S. C. Odewahn *et al.*, “The Digitized Second Palomar Observatory Sky Survey (DPOSS). III. Star-Galaxy Separation,” *The Astronomical Journal*, vol. 128, no. 6, pp. 3092–3107, Dec. 2004, doi: 10.1086/425525. [Online]. Available: http://dx.doi.org/10.1086/425525.

[147] W. Zheng *et al.*, “Five High-Redshift Quasars Discovered in Commissioning Imaging Data of the Sloan Digital Sky Survey,” *The Astronomical Journal*, vol. 120, no. 4, pp. 1607–1611, Oct. 2000, doi: 10.1086/301570. [Online]. Available: http://dx.doi.org/10.1086/301570.

[148] C. CUI et al., “Astronomy research in big-data era,” Chinese Science Bulletin (Chinese Version), vol. 60, no. 5–6, p. 445, 2015, doi: https://doi.org/10.1360/n972014-00839.

[149] K. Wang, P. Guo, F. Yu, L. Duan, Y. Wang, and H. Du, “Computational Intelligence in Astronomy: A Survey,” *International Journal of Computational Intelligence Systems*, Jan. 01, 2018. [Online]. Available: https://doi.org/10.2991/ijcis.11.1.43.

[150] J. R. P. Angel, P. Wizinowich, M. Lloyd-Hart, and D. Sandler, “Adaptive optics for array telescopes using neural-network techniques,” *Nature*, vol. 348, no. 6298, pp. 221–224, Nov. 1990, doi: 10.1038/348221a0. [Online]. Available: http://dx.doi.org/10.1038/348221a0.

[151] F.-M. . Hu and M.-H. . Jiang, “The fuzzy classification of the solar cycle and the prediction for the 22nd solar cycle.,” Chinese Journal of Space Science, vol. 5, pp. 237–244, Oct. 1985, [Online]. Available: https://ui.adsabs.harvard.edu/abs/1985ChJSS...5..237H/abstract.

[152] E. Eberbach, “Toward a theory of evolutionary computation,” Biosystems, vol. 82, no. 1, pp. 1–19, Oct. 2005, doi: https://doi.org/10.1016/j.biosystems.2005.05.006.

[153] “Anomalous Behavior Detection in Galaxies and Exoplanets using ML & DL Techniques,” ieeexplore.ieee.org. https://ieeexplore.ieee.org/document/9591860.

[154] “A Study of Light Intensity of Stars for Exoplanet Detection using Machine Learning,” ieeexplore.ieee.org. https://ieeexplore.ieee.org/document/9864366.

[155] “Exploring Exoplanets using kNN, Logistic Regression and Decision Trees,” ieeexplore.ieee.org. https://ieeexplore.ieee.org/document/9914278.

[156] R. Jagtap, U. Inamdar, S. Dere, M. Fatima, and N. B. Shardoor, “Habitability of Exoplanets using Deep Learning,” 2021 IEEE International IOT, Electronics and Mechatronics Conference (IEMTRONICS), Apr. 2021, doi: https://doi.org/10.1109/iemtronics52119.2021.9422571.

[157] I. Priyadarshini and V. Puri, “A convolutional neural network (CNN) based ensemble model for exoplanet detection,” Earth Science Informatics, Feb. 2021, doi: https://doi.org/10.1007/s12145-021-00579-5.

[158] “Detection and classification of exoplanets using hybrid kNN model,” ieeexplore.ieee.org. https://ieeexplore.ieee.org/document/9741029.

[159] Christopher J. Smith, Geronimo L. Villanueva, and Gabrielle Suissa. 2020. Imagining Exoplanets: Visualizing Faraway Worlds Using Global Climate Models. In ACM SIGGRAPH 2020 Talks (SIGGRAPH ’20). Association for Computing Machinery, New York, NY, USA, Article 20, 1–2. https://doi.org/10.1145/3388767.3407354.

[160] Michael Quinton, Iain McGregor, and David Benyon. 2020. Sonification of an exoplanetary atmosphere. In Proceedings of the 15th International Audio Mostly Conference (AM ’20). Association for Computing Machinery, New York, NY, USA, 191–198. https://doi.org/10.1145/3411109.3411117.

[161] Hatem Ltaief, Dalal Sukkari, Oliver Guyon, and David Keyes. 2018. Extreme Computing for Extreme Adaptive Optics: The Key to Finding Life Outside our Solar System. In Proceedings of the Platform for Advanced Scientific Computing Conference (PASC ’18). Association for Computing Machinery, New York, NY, USA, Article 1, 1–10. https://doi.org/10.1145/3218176.3218225.

[162] Yuyan Wang. 2021. The Identification of Transiting Exoplanet Candidates Based on Convolutional Neural Network. In Proceedings of the 2020 2nd International Conference on Big Data and Artificial Intelligence (ISBDAI '20). Association for Computing Machinery, New York, NY, USA, 5–8. https://doi.org/10.1145/3436286.3436288.

[163] A. Malik, B. P. Moster, and C. Obermeier, "Exoplanet detection using machine learning," Monthly Notices of the Royal Astronomical Society, https://doi.org/10.48550/arXiv.2011.14135.

[164] Shallue, C.J., & Vanderburg, A.M. (2017). Identifying Exoplanets with Deep Learning: A Five-planet Resonant Chain around Kepler-80 and an Eighth Planet around Kepler-90. The Astronomical Journal, 155. https://doi.org/10.48550/arXiv.1712.05044.

[165] Jin, Y., Yang, L., & Chiang, C. (2022). Identifying Exoplanets with Machine Learning Methods: A Preliminary Study. ArXiv, abs/2204.00721. https://doi.org/10.48550/arXiv.1907.11109.

[166] Chaushev, A., Raynard, L., Goad, M.R., Eigmuller, P., Armstrong, ¨ D.J., Briegal, J.T., Burleigh, M.R., Casewell, S.L., Gill, S., Jenkins, J.S., Nielsen, L.D., Watson, C.A., West, R.G., Wheatley, P.J., Udry, S., & Vines, J.I. (2019). Classifying exoplanet candidates with convolutional neural networks: application to the Next Generation Transit Survey. Monthly Notices of the Royal Astronomical Society. https://doi.org/10.48550/arXiv.2204.00721.

[167] J. P. Glaser, S. L. W. McMillan, A. M. Geller, J. D. Thornton, and M. R. Giovinazzi, "Tycho: Realistically Simulating Exoplanets within Stellar Clusters. I. Improving the Monte Carlo Approach," The Astronomical Journal, vol. 160, no. 3, p. 126, Aug. 2020, doi: https://doi.org/10.3847/1538-3881/aba2ea.